Title

Light-Driven Regeneration of Cone Visual Pigments through a Mechanism Involving RGR Opsin in Müller Glial Cells

Journal

Neuron, 102(6)

ISSN

0896-6273

Authors

Morshedian, Ala
Kaylor, Joanna J
Ng, Sze Yin
et al.

Publication Date

2019-06-01

DOI

10.1016/j.neuron.2019.04.004

Peer reviewed

Article

Neuron

Light-Driven Regeneration of Cone Visual Pigments through a Mechanism Involving RGR Opsin in Müller Glial Cells

Graphical Abstract

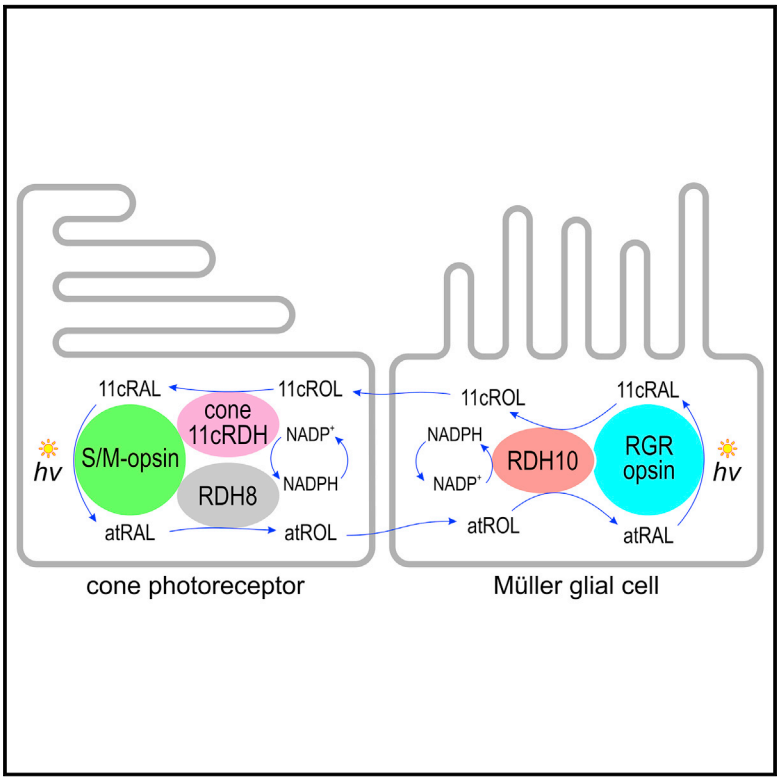

Authors

Ala Morshedian, Joanna J. Kaylor, Sze Yin Ng, ..., Roxana A. Radu, Gordon L. Fain, Gabriel H. Travis

Correspondence

travis@jsei.ucla.edu

In Brief

Morshedian et al. report that RGR opsin in Müller cells functions to regenerate cone visual pigments during light exposure and is the likely isomerase of the intrinsic retinal visual cycle. RGR opsin is required to maintain cone sensitivity during sustained light exposure.

Highlights

- RGR opsin and Rdh10 convert atROL to 11cROL upon exposure to visible light
- Normal mouse retinas maintain cone sensitivity during exposure to background light
- *Rgr*−/− mouse retinas progressively lose cone sensitivity during light exposure
- Treatment of normal mouse retinas with a Müller cell toxin replicates the *Rgr*−/− phenotype

Morshedian et al., 2019, Neuron *102*, 1172–1183
June 19, 2019
https://doi.org/10.1016/j.neuron.2019.04.004

CellPress

CellPress

Neuron
Article

Light-Driven Regeneration of Cone Visual Pigments through a Mechanism Involving RGR Opsin in Müller Glial Cells

Ala Morshedian,[1] Joanna J. Kaylor,[1] Sze Yin Ng,[1,2] Avian Tsan,[1] Rikard Frederiksen,[1] Tongzhou Xu,[1] Lily Yuan,[1] Alapakkam P. Sampath,[1] Roxana A. Radu,[1] Gordon L. Fain,[1,2] and Gabriel H. Travis[1,3,4,*]

[1]Stein Eye Institute and Department of Ophthalmology, University of California, Los Angeles, Los Angeles, CA, USA
[2]Department of Integrative Biology and Physiology, University of California, Los Angeles, Los Angeles, CA, USA
[3]Department of Biological Chemistry, University of California, Los Angeles, Los Angeles, CA, USA
[4]Lead Contact
*Correspondence: travis@jsei.ucla.edu
https://doi.org/10.1016/j.neuron.2019.04.004

SUMMARY

While rods in the mammalian retina regenerate rhodopsin through a well-characterized pathway in cells of the retinal pigment epithelium (RPE), cone visual pigments are thought to regenerate in part through an additional pathway in Müller cells of the neural retina. The proteins comprising this intrinsic retinal visual cycle are unknown. Here, we show that RGR opsin and retinol dehydrogenase-10 (Rdh10) convert all-*trans*-retinol to 11-*cis*-retinol during exposure to visible light. Isolated retinas from *Rgr*+/+ and *Rgr*−/− mice were exposed to continuous light, and cone photoresponses were recorded. Cones in *Rgr*−/− retinas lost sensitivity at a faster rate than cones in *Rgr*+/+ retinas. A similar effect was seen in *Rgr*+/+ retinas following treatment with the glial cell toxin, α-aminoadipic acid. These results show that RGR opsin is a critical component of the Müller cell visual cycle and that regeneration of cone visual pigment can be driven by light.

INTRODUCTION

Light perception in the retina begins with the absorption of a photon by an opsin visual pigment. The light-absorbing molecule in most animals is 11-*cis*-retinaldehyde (11cRAL), which is coupled to the opsin protein as a Schiff base and converted by light to the lower-energy isomer, all-*trans*-retinaldehyde (atRAL). The resulting change in opsin conformation activates its associated G protein and, thereby, the visual transduction cascade in both vertebrate and invertebrate photoreceptors. Rhabdomeric photoreceptors in the eyes of insects and other invertebrates contain bistable opsins where the atRAL remains covalently coupled to the protein following its activation (Fain et al., 2010). Absorption of a second photon converts the atRAL back to 11cRAL, which restores light sensitivity without the need for enzymatic synthesis of 11cRAL. In contrast, ciliary photoreceptors, such as rods and cones in the retinas of mammals, contain bleaching opsins that dissociate following light activation to yield free atRAL and unliganded apo-opsin. Light sensitivity is restored when apo-opsin combines with another 11cRAL to form a new visual pigment. Therefore, to sustain light sensitivity, ciliary photoreceptors must be supplied with chromophore at a rate that matches its rate of consumption through photoisomerization. Under dim light, this conversion is carried out in cells of the retinal pigment epithelium (RPE) by an enzyme pathway called the visual cycle. Under daylight conditions, however, photoisomerization of visual opsins in rods and cones far outstrips the synthesis of 11cRAL by this pathway (Mata et al., 2002). The mechanism whereby mammalian photoreceptors maintain light sensitivity under daylight conditions is unknown.

Accumulating evidence suggests the existence of a second visual cycle that regenerates cone visual pigments at least in part in the neural retina. Cones, but not rods, were shown to recover photosensitivity following light exposure in isolated retinas from multiple species, including humans and mice (Goldstein, 1970; Hood and Hock, 1973; Wang and Kefalov, 2009). Müller cells have been implicated in this process by several previous observations: (1) Müller cells express multiple retinoid-processing proteins, including cellular-retinaldehyde-binding protein (CRALBP, Bunt-Milam and Saari, 1983), cellular-retinol-binding protein-1 (CRBP1, Huang et al., 2009), retinol dehydrogenase-10 (Rdh10, Wu et al., 2004), retinol dehydrogenase-11 (Rdh11, Haeseleer et al., 2002), and retinol dehydrogenase-14 (Rdh14, Haeseleer et al., 2002); (2) cultured Müller cells take up atROL and release 11-*cis*-retinol (11cROL) into the medium (Betts-Obregon et al., 2014; Das et al., 1992); and (3) treatment of isolated retinas with the glial cell toxin, α-aminoadipic acid (α-AAA) (Jablonski and Iannaccone, 2000), abolished recovery of cone sensitivity in isolated retina (Wang and Kefalov, 2009). Because only 11cRAL can regenerate bleached opsin, these observations suggest further that cones, but not rods, contain an 11cROL dehydrogenase (11cRDH) activity that converts 11cROL to 11cRAL (Mata et al., 2002; Sato and Kefalov, 2016). Hence, the proposed Müller-cell visual cycle provides a ''private pipeline'' of chromophore precursor to regenerate cone opsin.

Cones are responsible for vision in bright light and operate at high rates of opsin photoisomerization. Recovery of cone sensitivity was shown to be limited by chromophore supply (Wang et al., 2014), emphasizing the importance of the retinal visual

cycle to cone function. Two proteins were tentatively identified as components of the Müller-cell visual cycle: dihydroceramide desaturase-1 (Des1) (Kaylor et al., 2013) and multifunctional *O*-acyltransferase (MFAT) (Kaylor et al., 2014). When co-expressed in cultured cells, Des1 and MFAT converted atROL to 11-*cis*-retinyl esters (11cREs), a lipid-soluble storage form of 11cROL. This "isomerosynthase" activity was also observed in homogenates of cone-dominant chicken and ground squirrel retinas but was undetectable in homogenates of rod-dominant mouse or cow retinas (Mata et al., 2002). Retinas from cone-dominant species contain 11cRE's, possibly due to Des1-MFAT activity, while 11cRE's were undetectable in rod-dominant retinas (Mata et al., 2002). Recent studies have shown that mice with a conditional null mutation of the *Des1* gene in Müller cells recover cone sensitivity normally (Kiser et al., 2019). For these reasons, Des1 probably plays no role in the regeneration of mouse cone opsin. RPE cells contain a retinoid isomerase (retinal pigment epithelium-specific 65-kDa protein or Rpe65) coupled to a retinyl-ester synthase (lecithin retinol acyltransferase or LRAT); however, neither Rpe65 nor LRAT is expressed in the neural retina (Kiser et al., 2019; Mata et al., 2005). Hence, the LRAT-Rpe65 isomerase system does not contribute to cone opsin regeneration in isolated retinas. The proteins responsible for 11cROL synthesis by Müller cells and the recovery of cone sensitivity in isolated retinas following a photobleach are hence unknown.

Retinal G protein-coupled receptor (RGR) opsin is a non-visual opsin in intracellular membranes of RPE and Müller cells (Pandey et al., 1994). In contrast to the visual opsins in photoreceptors, RGR opsin covalently binds atRAL in the dark, which is isomerized to 11cRAL upon exposure to light (Hao and Fong, 1999). Despite its name, RGR opsin lacks the conserved (E/D)R(Y/W/F) and NPxxY(x)$_{5,6}$F motifs required for interaction of a receptor with its G protein (Franke et al., 1992; Fritze et al., 2003). Thus, RGR is probably not a signaling molecule, consistent with its proposed role as a photoisomerase (Hao and Fong, 1999). Point mutations in the human *Rgr* gene are responsible for the inherited blinding disease retinitis pigmentosa (RP) in a small subset of cases (Morimura et al., 1999). Mice with a knockout mutation in the *Rgr* gene showed lower levels of rhodopsin and diminished rod b-wave amplitudes by *in vivo* electroretinography after exposure to bright light, suggesting that RGR plays a role in chromophore synthesis (Chen et al., 2001a). However, other studies on *Rgr*−/− mice found no light-dependent effects of RGR on rod photopigment regeneration (Maeda et al., 2003; Wenzel et al., 2005).

In this study, we present the first evidence for a role of RGR opsin in the regeneration of cone visual pigment. We show that RGR opsin functionally pairs with Rdh10 to carry out the light-dependent conversion of atROL to 11cROL. This activity was found in cultured cells expressing both RGR and Rdh10, and, in retinal fractions from normal, but not *Rgr*−/− mutant, mice lacking RGR opsin (Chen et al., 2001a). These findings suggest that RGR opsin and Rdh10 serve together as a light-dependent 11cROL generator. To test this possibility, we measured the sensitivity of cones in isolated retinas from normal and *Rgr*−/− mice during exposure to bright light. Cone responses in *Rgr*−/− retinas lost peak amplitude and sensitivity at a significantly faster rate than cones in *Rgr*+/+ retinas. A similar effect was seen in *Rgr*+/+ retinas following treatment with α-AAA. These results indicate that maintenance and recovery of cone responses in isolated mouse retinas requires a light-driven visual cycle that depends on RGR opsin. Thus, ciliary photoreceptors of vertebrates, like the rhabdomeric photoreceptors of invertebrates, can use light itself to regenerate visual pigment.

RESULTS

Coupled Photoisomerization and Oxidoreduction of Vitamin A by RGR Opsin and Rdh10

Müller cells take up atROL discharged by rods and cones during light exposure and release 11cROL to regenerate cone visual pigments (Betts-Obregon et al., 2014; Das et al., 1992; Mata et al., 2002). This activity could be carried out by RGR opsin in conjunction with a reversible retinol dehydrogenase with dual-substrate specificity. RGR opsin from bovine RPE was found to co-purify with retinol dehydrogenase-5 (Rdh5) (Simon et al., 1995), suggesting an interaction between these proteins (Chen et al., 2001b). However, Rdh5 is not expressed in the retina (Huang et al., 2009) and hence is an unlikely component of the retina visual cycle. In contrast, Rdh10 is present in both RPE and Müller cells (Wu et al., 2004). Further, Rdh10 exhibits dual-substrate specificity, favoring oxidation of atROL (Wu et al., 2002) and reduction of 11cRAL (Farjo et al., 2009). These properties suggest that RGR opsin and Rdh10 may cooperate in the presence of light to convert atROL to 11cROL. To test this possibility, we expressed bovine RGR opsin and Rdh10 alone and together in HEK293T cells. Cells were placed in assay media containing atROL and were maintained in darkness or exposed to UV-filtered white light (400-nm cutoff) for 30 min. Media and cells from each culture dish were extracted into hexane and analyzed for retinoid content by normal-phase high-performance liquid chromatography (HPLC). Low levels of 11cROL were observed in media from all cells maintained in darkness (Figure 1A). Similarly, media from light-exposed cells expressing RGR alone, Rdh10 alone, or neither protein also contained low 11cROL. However, media from cells co-expressing RGR opsin and Rdh10 and exposed to light contained dramatically higher 11cROL (Figure 1A). Chromatograms are shown in Figure S1. At the same time, levels of 11cRAL were not increased in media from light-exposed cells expressing RGR opsin and Rdh10 (Figure S2). These findings suggest close cooperativity between RGR opsin and Rdh10 such that 11cRAL produced by RGR photoisomerization is quantitatively reduced to 11cROL before it can escape into the media.

RGR Opsin and Rdh10 Interact Specifically

To test whether the interaction between RGR and Rdh10 is specific, we co-expressed RGR opsin in 293T cells with other retinol dehydrogenases from RPE and Müller cells. As before, we incubated these expressing 293T cells in media containing atROL and exposed the cells to UV-filtered white light. Negative controls included non-recombinant plasmid, RGR opsin alone, or Rdh10 alone. Cells expressing RGR opsin and Rdh10 from human, mouse, or chicken produced significant amounts of

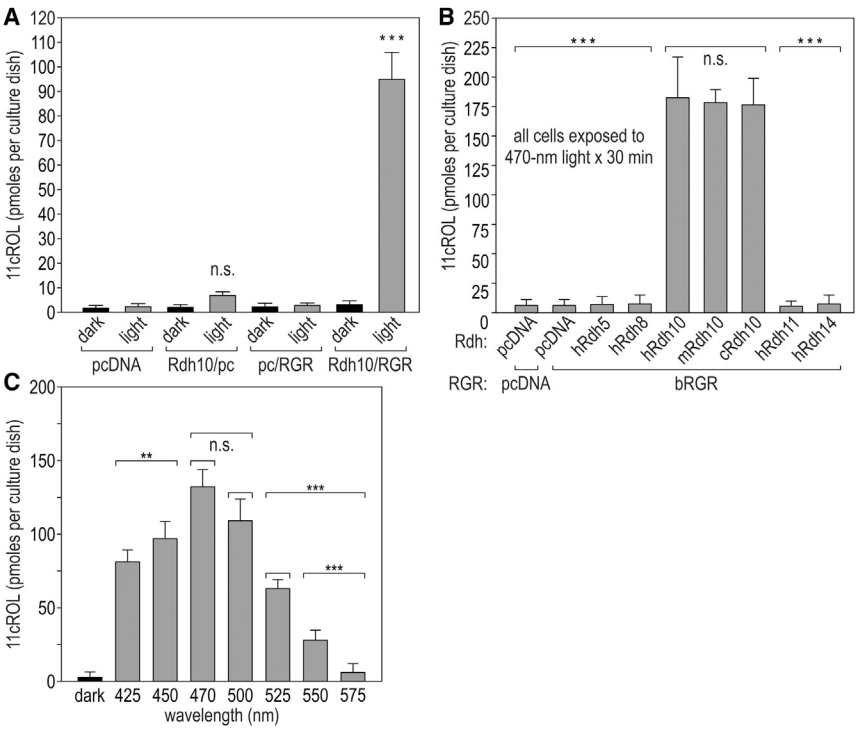

Figure 1. Production of 11cROL from atROL by RGR Opsin and Rdh10 in Cells Exposed to Light

(A) HEK293T cells were transfected with equal amounts of non-recombinant plasmid (pcDNA3.1) or plasmids containing the coding regions for Rdh10 (pcDNA3.1-bRdh10), RGR opsin (pcDNA3.1-bRGR), or both. After 2 days in culture to allow for protein expression, the culture media were supplemented with 5.0 μM atROL and 2% BSA under dim red light. Then, the cell cultures (~80% confluent) were incubated at 37°C for 30 min in the dark or exposed to monochromatic light (470 nm ± 10 nm at 0.2 W/m^2). Cell culture media were collected, extracted, and analyzed for retinoid content by normal-phase HPLC. Note the production of 11cROL only in media from light-exposed cells expressing both Rdh10 and RGR opsin ($p < 0.001$) relative to the other transfection and light-exposure conditions.

(B) HEK cells were transfected with non-recombinant plasmid (pcDNA3.1) alone, plasmid containing the coding region for RGR opsin plus pcDNA3.1, or plasmid containing the coding region for RGR opsin plus plasmid containing the coding region for Rdh5 (human), Rdh8 (human), Rdh10 (human, mouse, or chicken), Rdh11 (human), or Rdh14 (human), as indicated. After 2 days in culture, the culture media were supplemented with 5.0 μM atROL and 2% BSA under dim red light. Then, all cell cultures were incubated for 30 min during exposure to monochromatic light (470 nm ± 10 nm at 0.2 W/m^2). Culture media were collected, extracted, and analyzed by normal-phase HPLC for retinoid contents, expressed as pmoles per culture dish. Note the production of 11cROL ($p < 0.001$) in medium from cells expressing Rdh10 and RGR opsin, but not from cells expressing the other retinol dehydrogenases plus RGR opsin.

(C) Action spectrum of RGR and Rdh10. HEK293T cells were transfected with equal amounts of non-recombinant plasmid (pcDNA3.1) or plasmids containing the coding regions for Rdh10 (pcDNA3.1-bRdh10), RGR opsin (pcDNA3.1-bRGR), or both. After 2 days in culture, the media were supplemented with 5 μM atROL and 2% BSA under dim red light. The cell plates (~80% confluent) were exposed to monochromatic light (20-nm bandwidth) of wavelengths 425–575 nm for 30 min or maintained in darkness. The light intensities were adjusted to deliver the same photon flux at each wavelength (0.35 W/m^2 at 425 nm to 0.26 W/m^2 at 575 nm). The media above these plates were collected, extracted, and analyzed for retinoid contents, which are expressed as pmoles per mg total protein. Wavelengths between 425 and 525 nm showed increased production of 11-*cis*-retinol ($p < 0.01$) relative to cells maintained in darkness or the other monochromatic light wavelengths.

Each bar represents n = 3 plates of transfected cells. Data represent mean ± SD; n.s., not significant, *$p < 0.05$, **$p < 0.01$, ***$p < 0.001$, one-way ANOVA with Tukey's post hoc analysis.

11cROL (Figure 1B). In contrast, cells expressing RGR opsin alone or RGR plus Rdh5, Rdh8, Rdh11, or Rdh14 produced only background levels of 11cROL. These data indicate that Rdh10 interacts selectively with RGR opsin to convert atROL into 11cROL, although Rdh11-Rdh14 also act on 11c- and at-retinoids (Haeseleer et al., 2002). Similar rates of 11cROL formation were observed with Rdh10's from mouse, human, or chicken (Figure 1B), indicating similar activities of the three homologs. Therefore, the redox photoisomerase activity of RGR opsin is specific to Rdh10.

The Action Spectrum of RGR Photoisomerase Activity Corresponds to Its Absorption Spectrum

RGR opsin combined with atRAL exhibits absorption maxima (λ_{max}) at 375 and 466 nm, corresponding to non-protonated and protonated forms of the retinylidene Schiff base (Hao and Fong, 1996). Since the ocular medium blocks transmittance of light below 400 nm in humans (Boettner and Wolter, 1962), only protonated RGR opsin may function *in vivo* as a retinaldehyde photoisomerase. To confirm that RGR opsin is responsible for the light-dependent conversion of atROL to 11cROL, we repeated the assays on cells expressing RGR and Rdh10 with monochromatic light (20-nm bandwidth) of wavelengths 425-to-575 nm. Light intensities were adjusted to yield equal photon fluxes at each wavelength. Other plates of expressing cells were exposed to UV-filtered full-spectrum light or were maintained in darkness, as positive and negative controls. After incubating the live cells for 30 min in the presence of atROL, we extracted the culture media and determined the retinoid content by HPLC. Synthesis of 11cROL by these cells varied strongly with light conditions (Figure 1C). Again, we observed only background 11cROL in media from expressing cells incubated in darkness. Of cultures exposed to narrow-band light, the highest synthesis of 11cROL occurred at 470 nm, with reduced synthesis at longer and shorter wavelengths (Figure 1C). This action spectrum for 11cROL synthesis by RGR-expressing cells overlaps the absorption spectrum of protonated RGR opsin (Hao and Fong, 1996), providing further evidence that all-*trans* (at) to 11-*cis* (11c) retinoid photoisomerization was carried out by RGR opsin in these cells.

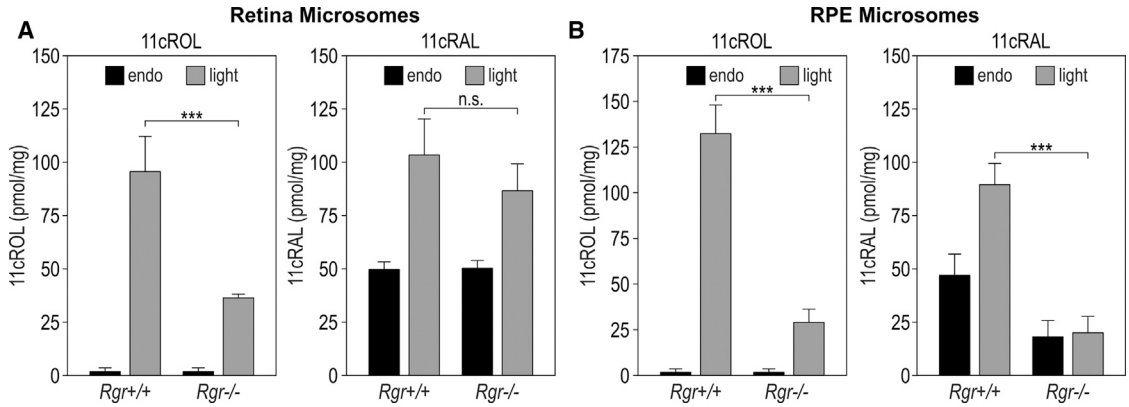

Figure 2. Conversion of atROL to 11cROL and 11cRAL by Light-Exposed Microsomes from Wild-type and *Rgr*–/– Retinas and RPE

Retinas and RPE-containing eyecups were collected from 2-month-old *Rgr*+/+ (129/Sv) and *Rgr*−/− mice. Microsomes were prepared from each tissue. The samples were supplemented with 2% BSA and 5 μM atROL. One set of samples was extracted to determine the endogenous retinoid content (endo). The remaining samples were placed in cuvettes and agitated during exposure to 470-nm monochromatic light (20-nm bandwidth) at 0.2 W/m^2 for 30 min at 37°C (light). Retinoids were extracted and analyzed by normal-phase HPLC.

(A) 11cROL and 11cRAL synthesized by retina microsomes from WT and *Rgr*−/− mice is expressed as pmoles per mg total protein. Note the several-fold reduction in 11cROL ($p < 0.001$) and unchanged 11cRAL produced by *Rgr*−/− versus WT retina microsomes in light.

(B) 11cROL and 11cRAL synthesized by RPE microsomes from *Rgr*+/+ and *Rgr*−/− mice expressed as pmoles per mg total protein. Note the several-fold reduction in both 11cROL and 11cRAL produced by *Rgr*−/− versus WT RPE microsomes in light ($p < 0.001$).

Each bar represents n = 3 samples of microsomes. Data represent mean ± SD; n.s., not significant, *$p < 0.05$, **$p < 0.01$, ***$p < 0.001$, one-way ANOVA with Tukey's post hoc analysis.

Redox-Photoisomerase Activity in Mouse Retina and RPE Microsomes

If light-dependent conversion of atROL to 11cROL by expressing HEK cells mirrors the *in vivo* activity of Rdh10 and RGR, similar redox-photoisomerase activity should be present in retinas. To test this possibility, we prepared microsomal membranes from wild-type (WT) (*Rgr*+/+) and *Rgr*−/− mouse retinas and RPE-containing eyecups (see STAR Methods). Microsomes from *Rgr*+/+ mouse retinas produced 2.7-fold greater 11cROL during light exposure than did *Rgr*−/− retina microsomes (Figure 2A). In contrast, we observed no significant difference in levels of 11cRAL between *Rgr*+/+ and *Rgr*−/− retina microsomes. The endogenous 11cRAL in *Rgr*+/+ and *Rgr*−/− retina microsomes is from unbleached rhodopsin and cone-opsin pigments in these membrane samples (Figure 2A). The increased 11cRAL following light exposure, which occurred independent of RGR opsin, probably reflects at- to 11c-photoisomerization of *N*-ret-PE (Kaylor et al., 2017). These results corroborate our observations that light and RGR can mediate production of 11cROL by HEK cells expressing RGR and Rdh10 (Figure 1A).

Since RGR opsin and Rdh10 are also both present in RPE internal membranes (Chen et al., 2001b; Pandey et al., 1994), we tested for redox photoisomerase activity in microsomes from *Rgr*+/+ and *Rgr*−/− mouse RPE. Here, we observed nearly 5-fold-greater production of 11cROL by light-exposed *Rgr*+/+ versus *Rgr*−/− RPE microsomes (Figure 2B), suggesting that RGR opsin and Rdh10 in the RPE also exhibit redox-photoisomerase activity. In contrast to retina microsomes, we observed several-fold-lower 11cRAL production in dark- and light-exposed RPE microsomes from *Rgr*−/− versus *Rgr*+/+ mice (Figure 2B). This can be explained by the three-fold-lower Rpe65-isomerase activity in RPE homogenates from *Rgr*−/− versus *Rgr*+/+ mice (Radu et al., 2008; Wenzel et al., 2005).

The conversion of atROL to 11cROL carried out by mouse retina and RPE microsomes (Figures 2A and 2B) was observed with no dinucleotide cofactor added to the assay mixtures. Because microsomal membranes are depleted of cytoplasmic contents, these findings suggest that NADPH/NADP$^+$ cofactor may remain in association with Rdh10, switching between reduced and oxidized forms with oxidation of atROL and reduction of 11cRAL.

RGR Opsin Is Expressed in Müller Cells of the Mouse Retina

Although RGR opsin has been shown to be expressed in Müller cells of human (Trifunovic et al., 2008), bovine (Pandey et al., 1994), and chicken retinas (Díaz et al., 2017), it has not been detected in cells of the mouse retina (Tao et al., 1998; Trifunovic et al., 2008). To establish that RGR opsin is expressed in mouse retinas, we collected neural retinas and RPE-containing eyecups from *Rgr*+/+ (129/Sv) and *Rgr*−/− mice, prepared protein homogenates from these tissues, and analyzed them by immunoblotting with an antibody against mouse RGR opsin. Immunoreactive bands corresponding to RGR opsin were present in lanes containing isolated neural retinas and RPE-containing eyecups (Figure 3A). To establish RGR opsin expression in mouse Müller cells, we performed immunofluorescence analysis on thick (18-μm) retina sections from *Rgr*+/+ and *Rgr*−/− mice. As a control, we used antibodies against CRALBP, which is also expressed in RPE and Müller cells. RGR opsin and CRALBP co-localized in Müller cell endfeet, the inner nuclear layer

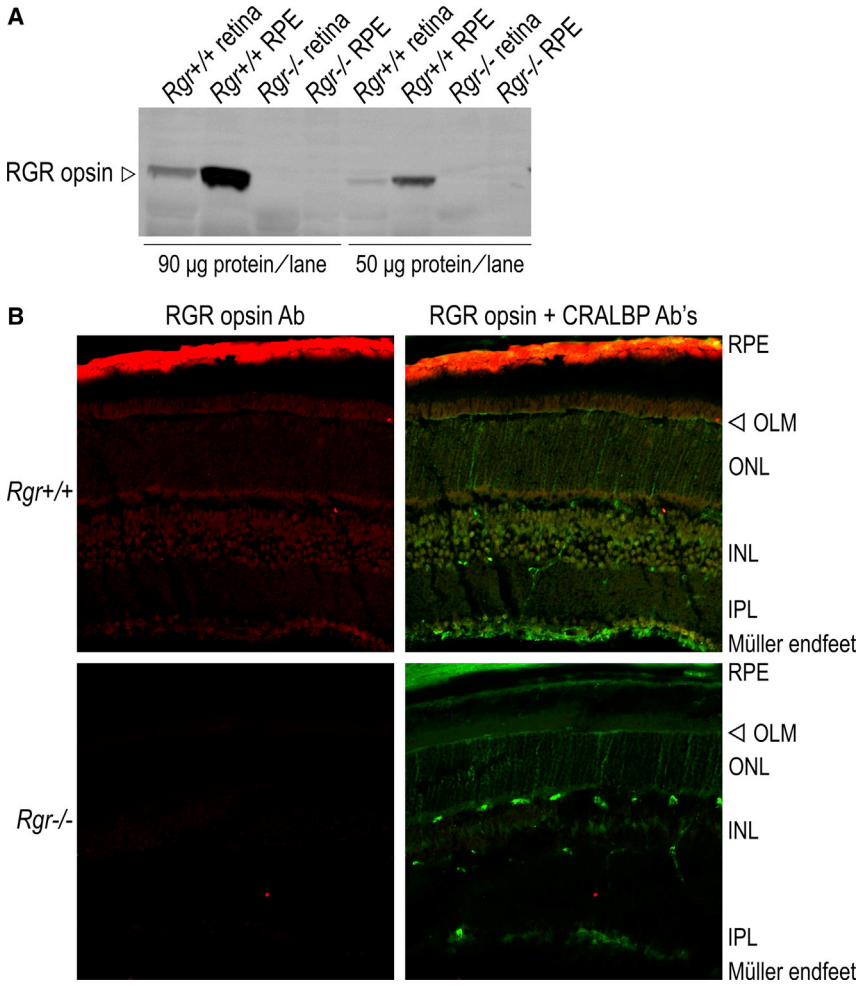

Figure 3. RGR Opsin Is Expressed in Mouse Müller Cells

(A) Representative immunoblot containing homogenates of neural retinas (retina) and RPE-containing eyecups (RPE) from *Rgr*+/+ and *Rgr*−/− mice. The blot was probed with the anti-RGR opsin (Pin 2) antibody. Lanes were loaded with 90 or 50 µg total protein as indicated.

(B) Immunofluorescence analysis of RGR opsin and CRALBP in 18-µm retina sections from *Rgr*+/+ and *Rgr*−/− mice. Sections were probed with rabbit polyclonal anti-RGR Pin3 (red) and mouse monoclonal anti-RLBP1 clone 1H7 (CRALBP, green). Images were acquired on an Olympus FluoView FV1000 confocal microscope under a 40x oil objective. Note the co-localization of RGR opsin and CRALBP in Müller-cell endfeet, the inner nuclear layer (INL) and in the apical microvilli of Müller cells above the outer limiting membrane (OLM).

containing Müller-cell nuclei, and in the apical microvilli of Müller cells above the outer limiting membrane (Figure 3B). Importantly, we observed no RGR immunoreactivity in retinas from *Rgr*−/− mice (Figure 3B). These data confirm that RGR opsin is expressed in mouse Müller cells.

Contribution of RGR Opsin to the Cone Photoresponse under Continuous Illumination

If the atROL to 11cROL redox-photoisomerase activity of Rdh10 and RGR opsin plays a role in vision, loss of RGR opsin should affect cone function during light exposure. To explore this possibility, we crossed the *Rgr*−/− mutation onto the *Gnat1*−/− background to yield *Rgr*−/− *Gnat1*−/− mice with absent rod but normal cone photoresponses (Calvert et al., 2000; Chen et al., 2001a). Isolated retinas (without the RPE) were collected and placed individually into a specially designed recording chamber that has been shown to support cone photoresponses for several hours (Vinberg et al., 2014). The retinas were perfused with a medium containing synaptic inhibitors to suppress responses from retinal interneurons and glial cells (Vinberg et al., 2014; Wang and Kefalov, 2009), and 10 µM atROL, to maintain constant substrate concentration during the recordings. Cone photoresponses were elicited with test flashes at 565 nm, which photoisomerizes M opsin (λ_{max} = 508 nm) with 10^7-fold-greater efficiency than S opsin (λ_{max} = 357 nm) (Govardovskii et al., 2000). Recordings were made in dark-adapted retinas immediately before and at various times during continuous exposure to 505-nm background light at an intensity of 9.1 × 10^6 photons (ϕ) μm^{-2} s^{-1}, estimated to bleach 10^6 M-opsin pigment molecules per second (10^6 P* s^{-1}) (see STAR Methods).

Representative recordings from *Rgr*+/+ *Gnat1*−/− retinas are shown in Figure 4A. Under continuous light, cone responses gradually diminished in sensitivity and maximum amplitude during the 1-h recording period. In the absence of any pigment regeneration, the background light can be calculated to bleach essentially all the M-opsin pigment during the 1-h exposure, leaving less than a single unbleached pigment molecule per cone. A bleach of this magnitude would be expected to produce dramatically lower response amplitudes than those observed (Figure 4A), suggesting concurrent regeneration of M opsin in *Rgr*+/+ *Gnat1*−/− retinas during light exposure. To test whether RGR opsin contributes to cone regeneration, we repeated the experiment using retinas from *Rgr*−/− *Gnat1*−/− mice. Here, we observed more rapid loss of cone response amplitude (Figure 4B). These results suggest that, under continuous illumination, retinas lacking RGR undergo faster net bleaching of cone opsins. Next, we pre-incubated *Rgr*+/+ *Gnat1*−/− retinas in a medium containing 10 mM α-AAA. This potent gliotoxin acts by inhibiting the glutamate transporter and glutamine synthetase in Müller cells (Jablonski and Iannaccone, 2000; McBean, 1994). Pre-incubation with α-AAA was shown to block recovery of cones in isolated mouse retinas (Wang and Kefalov, 2009). We recorded cone photoresponses in α-AAA-treated *Rgr*+/+ *Gnat1*−/− retinas during light exposure. These retinas exhibited rapid loss of cone response amplitude (Figure 4C), similar to

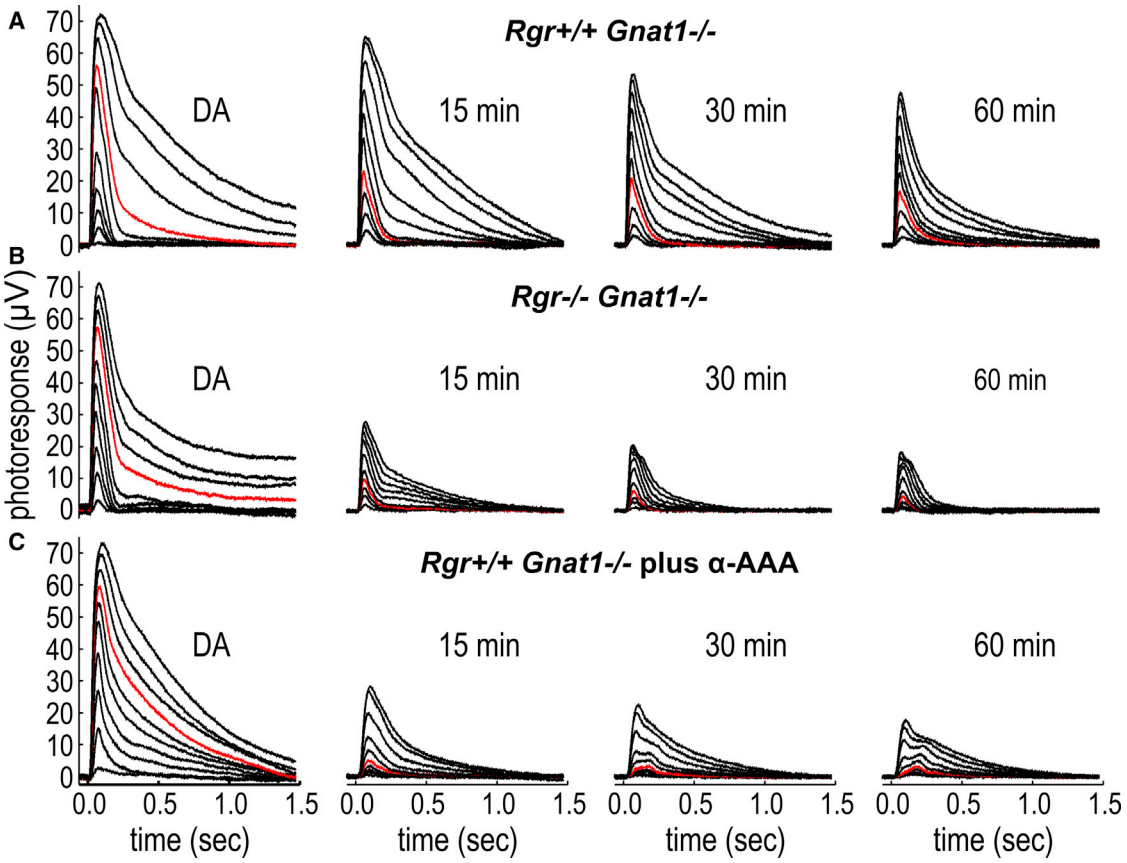

Figure 4. Representative Transretinal Responses of (A) *Rgr*+/+ *Gnat1*–/– mice, (B) *Rgr*–/– *Gnat1*–/– mice, and (C) *Rgr*+/+ *Gnat1*–/– Mice Incubated with α-AAA

M-Cone isolated photoreceptor recordings were made in dark-adapted (DA) retinas and after 15, 30, and 60 min of exposure to a continuous 505-nm background light (9.1×10^{6} ϕ μm^{-2} s^{-1}). The stimulating light flashes were produced by a 565-nm LED (flashes ranging from 65 ϕ μm^{-2} to 5.4×10^{7} ϕ μm^{-2} effective at the λ_{max} of the M cone pigment). Red traces show responses to a constant flash of an intensity of 3.7×10^{5} ϕ μm^{-2}. Note the lower response amplitudes in *Rgr*−/− versus *Rgr*+/+ retinas or when isolated *Rgr*+/+ retinas were incubated in α-AAA.

untreated *Rgr*−/− *Gnat1*−/− retinas (Figure 4B). Thus, loss of RGR opsin, due to a mutation in its gene or pharmacological ablation of Müller cells, results in diminished cone-response amplitude and sensitivity during light exposure.

Effect of RGR Opsin on Cone Sensitivity

The effect of RGR opsin on cone sensitivity was quantified by plotting response amplitudes in Figure 4 against the number of photons (ϕ) contained in each of the flashes. Figures 5A–5C show response-intensity curves as a function of duration of background exposure for the three conditions in Figure 4. The curves have been fitted with the Hill Equation (Equation 1),

$$r = \frac{r_{max} I^{n}}{I^{n} + I_{1/2}^{n}} \qquad \text{(Equation 1)}$$

where r is the amplitude of the response, r_{max} is the maximum response amplitude, I is the number of incident 565-nm photons in the flash (ϕ μm^{-2}), and n is an exponent. Best-fitting values of r_{max} and n are given in the Figure 5. The curves were shifted to the right and downward from the decrease in sensitivity and maximum amplitude, initially as a result of adaptation of the cones to the background light (see Figure S3; Burkhardt, 1994). The curves continued to shift and decrease in maximum amplitude, presumably from bleaching of pigment and gradual loss of chromophore during perfusion of the retina despite the addition of atROL to the medium. In the absence of RGR, or after exposure of the retina to α-AAA, the curves were dramatically shifted further downward and to the right (Figures 5B and 5C). These changes in sensitivity and response amplitude are compared in Figures 5D and 5E. No significant changes in sensitivity or response amplitude were observed over the 60-min recording duration when retinas were maintained in darkness. Sensitivities were significantly lower in *Rgr*−/− *Gnat1*−/− retinas and *Rgr*+/+ *Gnat1*−/− retinas treated with α-AAA compared to *Rgr*+/+ *Gnat1*−/− control retinas (see Figure 5 and STAR Methods). No significant differences were detected between untreated *Rgr*−/− *Gnat1*−/− and α-AAA-treated *Rgr*+/+ *Gnat1*−/− retinas.

Post-Bleach Recovery of Cone Sensitivity in the Dark

Conversion of atROL to 11cROL by cells expressing Rdh10 and RGR was only observed following exposure to light (Figures 1A

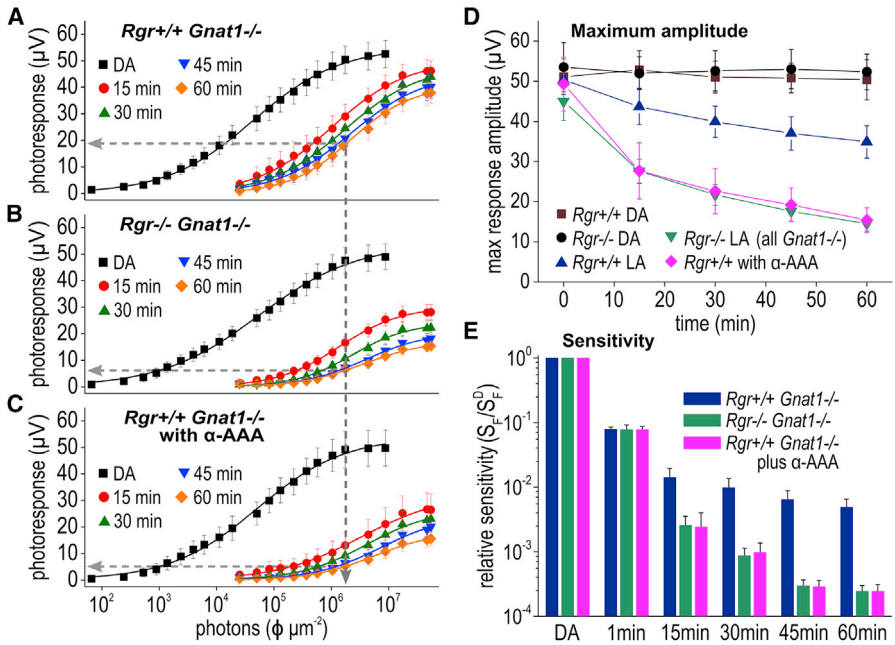

Figure 5. The Effect of RGR and Müller Cells on Intensity-Response Relations, Photosensitivity and Maximum Response Amplitude of M-Cones in *Rgr*+/+ *Gnat1*−/−, *Rgr*−/− *Gnat1*−/−, and *Rgr*+/+ *Gnat1*−/− Retinas Incubated in α-AAA in the Presence of a Continuous Light

(A–C) Changes in the intensity-response relations in dark-adapted retinas from mice of the indicated genotypes at 15 min, 30 min, 45 min, and 60 min in the presence of a continuous light (9.1×10^6 ϕ μm^{-2} s^{-1}), plotted as a function of incident photons from mouse cones in (A) *Rgr*+/+ *Gnat1*−/− (n = 9), (B) *Rgr*−/− *Gnat1*−/− (n = 8), and (C) *Rgr*+/+ *Gnat1*−/− incubated with α-AAA (n = 5). Curves are best fits to the Hill equation (Equation 1) with the following parameter values: (A) V_{max} = 55.1, $I_{1/2} = 4.4 \times 10^4$, n = 0.58 (DA); V_{max} = 50.0 and $I_{1/2} = 1.0 \times 10^6$, n = 0.66 (15 min); V_{max} = 48.0, $I_{1/2} = 1.7 \times 10^6$, n = 0.66 (30 min); V_{max} = 45.3 $I_{1/2} = 2.2 \times 10^6$, n = 0.67 (45 min); V_{max} = 40.0, $I_{1/2} = 2.1 \times 10^6$, n = 0.81 (60 min); (B) V_{max} = 53.0, $I_{1/2} = 4.9 \times 10^4$, n = 0.52 (DA); V_{max} = 30.2 and $I_{1/2} = 1.4 \times 10^6$, n = 0.79 (15 min); V_{max} = 23.9, $I_{1/2} = 2.3 \times 10^6$, 0.88 (30 min); V_{max} = 20.5, $I_{1/2} = 3.9 \times 10^6$, n = 0.80 (45 min), and V_{max} = 17.3, $I_{1/2} = 3.7 \times 10^6$ n = 0.79 (60 min); and (C) V_{max} = 55.1, $I_{1/2} = 4.7 \times 10^4$, n = 0.57 (DA); V_{max} = 32.4 and $I_{1/2} = 3.3 \times 10^6$, 0.59 (15 min); V_{max} = 26.6, $I_{1/2} = 4.0 \times 10^6$, n = 0.74 (30 min); V_{max} = 24.6, $I_{1/2} = 5.4 \times 10^6$, n = 0.73 (45 min); V_{max} = 18.2, $I_{1/2} = 5.6 \times 10^6$, n = 0.79 (60 min). Half-maximal response amplitude of the *Rgr*+/+ *Gnat1*−/− at 60 min is shown with a dashed line in (A). The same flash intensity generates significantly smaller responses at 60 min in *Rgr*−/− *Gnat1*−/− and *Rgr*+/+ *Gnat1*−/− incubated with α-AAA.

(D) Mean maximum response amplitude and (E) relative dim flash sensitivity from recordings of Figure 4 were calculated and plotted (with SE) as a function of time. Maximum amplitudes were significantly smaller (see STAR Methods) in *Rgr*−/− *Gnat1*−/− retinas than in *Rgr*+/+ *Gnat1*−/− retinas ($p < 10^{-9}$). That was also true for *Rgr*+/+ *Gnat1*−/− retinas and retinas treated with α-AAA acid ($p < 2 \times 10^{-6}$). There was no significant difference between *Rgr*−/− *Gnat1*−/− or *Rgr*+/+ *Gnat1*−/− α-AAA-treated retinas (p = 0.85). No significant change in response amplitude could be detected when either *Rgr*+/+ *Gnat1*−/− or *Rgr*−/− *Gnat1*−/− retinas were kept in darkness.

(E) Sensitivities were significantly lower in *Rgr*−/− *Gnat1*−/− retinas ($p < 8.2 \times 10^{-4}$) or retinas treated with α-AAA acid ($p < 0.009$). No significant difference could be detected between *Rgr*−/− *Gnat1*−/− and *Rgr*+/+ *Gnat1*−/− α-AAA-treated retinas (p = 0.83).

and 1C), suggesting that RGR opsin has no isomerase activity in the dark. An earlier study showed dark recovery of cones in isolated *Gnat1*−/− mouse retinas following a deep photobleach, which was interpreted to support the existence of a "dark" isomerase in Müller cells, however (Wang and Kefalov, 2009). To understand this apparent discrepancy, we repeated the published experiment (Wang and Kefalov, 2009) using an identical 30-s illumination calculated to bleach ~90% of mouse M-opsin pigment in isolated *Rgr*+/+ *Gnat1*−/− and *Rgr*−/− *Gnat1*−/− retinas, followed by incubation in darkness. Substantially lower recovery of cone sensitivity was seen in *Rgr*−/− *Gnat1*−/− retinas (Figure 6). Both retinas showed an initial, approximately 3-fold gain in sensitivity immediately after the bleach, probably due to dark adaptation of the visual transduction cascade (Figure S3) versus regeneration of cone opsin. Recovery thereafter was significantly different, and after 60 min the *Rgr*−/− *Gnat1*−/− retinas exhibited ~10-fold lower cone sensitivity than the *Rgr*+/+ *Gnat1*−/− retinas.

Regeneration of a cone opsin pigment by RGR opsin and Rdh10 in Müller cells requires multiple steps: (1) dissociation of bleached cone opsin, (2) reduction of atRAL to atROL by Rdh8, (3) transit of atROL from cone to Müller cell, (4) oxidation of atROL to atRAL by Rdh10, (5) photoisomerization of atRAL to 11cRAL by RGR opsin, (6) reduction of 11cRAL to 11cROL by Rdh10, (7) transit of 11cROL from Müller cell to cone, (8) oxidation of 11cROL to 11cRAL by the unidentified cone 11cRDH, and (9) conversion of apo-opsin to cone opsin pigment by recombination with 11cRAL. Because these events take time to complete, and the amount of RGR opsin in Müller cells may be limiting, short exposure of a retina to bright light might have a different effect from long exposure to dim light conveying similar total photons. To test this possibility, we repeated the experiment of Figure 6 on *Rgr*+/+ *Gnat1*−/− retinas with a much brighter light of shorter duration calculated to bleach the same 90% of M-opsin in 350 ms instead of in 30 s. Here, we observed much less RGR-dependent recovery of cone sensitivity (blue

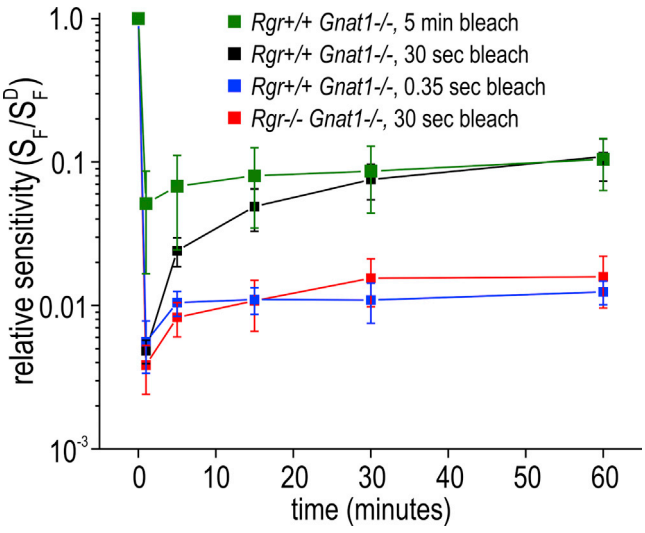

Figure 6. The Role of RGR in Dark Adaptation

Time dependence of normalized M-cone sensitivity following a 565-nm light exposure calculated to bleach 90% of the cone photopigment. The following animals were used for bleach exposures with the following durations (the intensity of the bleaching light was adjusted to give the same calculated bleach): *Rgr*+/+ *Gnat1*−/− with 30-s stimulus (n = 8), *Rgr*−/− *Gnat1*−/− with 30-s stimulus (n = 5), *Rgr*+/+ *Gnat1*−/− with 350-ms stimulus (n = 5), and *Rgr*+/+ *Gnat1*−/− with 5-min stimulus (n = 5). Post-bleach recovery of sensitivity was significantly different between *Rgr*−/− *Gnat1*−/− bleached in 30 s and *Rgr*+/+ *Gnat1*−/− bleached in 30 s ($p < 8.6x10^{-4}$, see STAR Methods) or *Rgr*+/+ *Gnat1*−/− bleached in 5 min ($p < 7.8x10^{-4}$). The duration of the bleach also affected the recovery of sensitivity. *Rgr*+/+ *Gnat1*−/− bleached with the 350-ms stimulus showed significantly smaller recovery compared to *Rgr*+/+ *Gnat1*−/− bleached with the 30-s stimulus ($p < 6.3x10^{-4}$). There was however no significant difference between *Rgr*+/+ *Gnat1*−/− bleached with the 350-ms stimulus and *Rgr*−/− *Gnat1*−/− bleached in 30 s ($p = 0.66$) . Also, there was no significant difference between *Rgr*+/+ *Gnat1*−/− bleached in 30s and *Rgr*+/+ *Gnat1*−/− bleached in 5 min ($p = 0.35$).

squares, Figure 6). There was no significant difference in the recovery of sensitivity (see legend to Figure 6 and STAR Methods) between *Rgr*+/+ *Gnat1*−/− bleached in 350 ms (blue squares) and *Rgr*−/− *Gnat1*−/− retinas bleached in 30 seconds (red squares), indicating the essential role of RGR opsin in sensitivity recovery. We also repeated the experiment on *Rgr*+/+ *Gnat1*−/− retinas with a dimmer light calculated to bleach 90% of M-opsins in 5 min. Recovery after 1 min was much greater than with the 30-s bleach, perhaps because the intensity of the bleaching light was ten-fold dimmer, but recovery was not significantly different at the other times at which it was measured.

Effect of *N*-ret-PE Photoisomerization on the Cone Photoresponse under Continuous Illumination

N-retinylidene phosphatidylethanolamine (*N*-ret-PE) is a conjugate of retinaldehyde and PE in OS disks. *N*-ret-PE occurs in the same stereoisomeric configurations as retinaldehyde. Recently, at-*N*-ret-PE was shown to undergo specific photoisomerization to 11c-*N*-ret-PE upon exposure to blue light (Kaylor et al., 2017). Further, 11c-*N*-ret-PE efficiently donated its 11cRAL to bleached opsin, regenerating visual pigments in rods and cones (Kaylor et al., 2017). To compare the contributions of *N*-ret-PE- and RGR-photoisomerization to pigment regeneration, we took advantage of the difference in the visible absorption spectra between *N*-ret-PE (λ_{max} = 450 nm) and M-opsin (λ_{max} = 508 nm). While the photosensitivity of M-opsin is similar at 450 and 560 nm (Govardovskii et al., 2000), the photosensitivity of *N*-ret-PE is nearly 30-fold higher at 450 versus 560 nm (Kaylor et al., 2017). Accordingly, we measured cone photoresponses to flash families in retinas from *Rgr*+/+ *Gnat1*−/− and *Rgr*−/− *Gnat1*−/− mice during exposure to monochromatic background light at 450 or 560 nm. Cone responses in *Rgr*+/+ *Gnat1*−/− retinas exposed to 450-nm background light declined slowly over 60 min (Figure 7A), reflecting the contributions of both RGR opsin and *N*-ret-PE photoisomerization to pigment regeneration. Cone responses in *Rgr*−/− *Gnat1*−/− retinas exposed to 450-nm light showed a faster decline (Figure 7B). The responses here reflect M-opsin regeneration through photoisomerization of *N*-ret-PE but not RGR opsin. Finally, we measured cone photoresponses in *Rgr*−/− *Gnat1*−/− retinas during exposure to 560-nm background light (Figure 7C). The responses here reflect cone pigment regeneration with minimal contributions from RGR opsin or *N*-ret-PE. The maximum cone-response amplitudes at various times during the 60-min light exposures are shown in Figure 7D, while cone sensitivities calculated from the same recordings are shown in Figure 7E. Both the cone sensitivity and maximum amplitude were significantly lower in retinas illuminated with the 560-nm light (Figure 7 and STAR Methods). Mean intensity-response curves for these experiments are shown in Figure S4. These results suggest that photoisomerization of RGR opsin and *N*-ret-PE both contribute to cone recovery.

DISCUSSION

This work describes a new mechanism for the regeneration of cone visual pigment. Illumination of RGR opsin in cells that also express Rdh10 results in the conversion of atROL to 11cROL. Since bleached cones, but not rods, can recover light sensitivity upon addition of 11cROL (Jones et al., 1989), production of 11cROL by RGR-Rdh10 allows cones to escape competition from rods for limited chromophore in bright light. If RGR opsin affects light-dependent regeneration of cone visual pigment, cone function should be impaired in light-exposed retinas from *Rgr*−/− mice. To test this possibility, we generated *Rgr*−/− *Gnat1*−/− double-mutant mice that lack both RGR opsin and rod α-transducin. Cone responses were similar in dark-adapted retinas of the two genotypes (Figure 4). However, striking differences were observed between retinas that express or lack RGR opsin when recordings were made under continuous background illumination. While *Rgr*+/+ retinas exhibited only gradual loss of cone sensitivity under constant background light, *Rgr*−/− retinas lost cone sensitivity much more rapidly (Figure 5). These observations indicate that RGR opsin contributes to sustained cone vision under daylight conditions.

Co-expression of RGR opsin and Rdh10 yielded a novel catalytic activity that converts atROL to 11cROL upon exposure to visible light (Figure 1A). Following photoisomerization, the 11cRAL product remains bound to the RGR opsin protein (Chen et al., 2001b). This restriction on RGR turnover is overcome

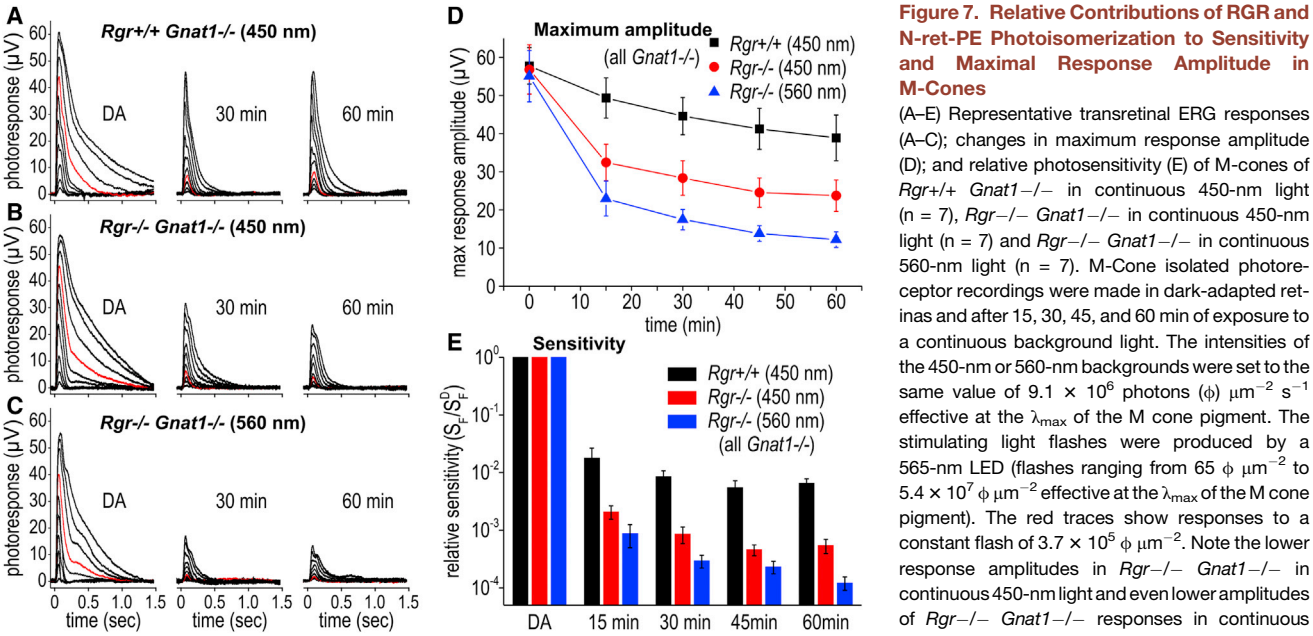

Figure 7. Relative Contributions of RGR and N-ret-PE Photoisomerization to Sensitivity and Maximal Response Amplitude in M-Cones

(A–E) Representative transretinal ERG responses (A–C); changes in maximum response amplitude (D); and relative photosensitivity (E) of M-cones of *Rgr*+/+ *Gnat1*−/− in continuous 450-nm light (n = 7), *Rgr*−/− *Gnat1*−/− in continuous 450-nm light (n = 7) and *Rgr*−/− *Gnat1*−/− in continuous 560-nm light (n = 7). M-Cone isolated photoreceptor recordings were made in dark-adapted retinas and after 15, 30, 45, and 60 min of exposure to a continuous background light. The intensities of the 450-nm or 560-nm backgrounds were set to the same value of 9.1 × 10^6 photons (ϕ) μm^{-2} s^{-1} effective at the λ_{max} of the M cone pigment. The stimulating light flashes were produced by a 565-nm LED (flashes ranging from 65 ϕ μm^{-2} to 5.4 × 10^7 ϕ μm^{-2} effective at the λ_{max} of the M cone pigment). The red traces show responses to a constant flash of 3.7 × 10^5 ϕ μm^{-2}. Note the lower response amplitudes in *Rgr*−/− *Gnat1*−/− in continuous 450-nm light and even lower amplitudes of *Rgr*−/− *Gnat1*−/− responses in continuous 560-nm light. Mean maximum response amplitude (D) and relative dim flash sensitivity (E) of individual recordings in (A), (B), and (C) are calculated and plotted (with SE) as a function of time. The maximum amplitudes were significantly lower in *Rgr*−/− *Gnat1*−/− retinas in 450-nm light ($p < 0.001$) and *Rgr*−/− *Gnat1*−/− at 560-nm ($p < 10^{-7}$) compared to *Rgr*+/+ *Gnat1*−/− at 450-nm. The maximum amplitudes were also significantly lower in *Rgr*−/− *Gnat1*−/− retinas in 450-nm light compared to *Rgr*−/− *Gnat1*−/− retinas in 560-nm light ($p < 8.4 \times 10^{-4}$). The sensitivities were significantly lower in *Rgr*−/− *Gnat1*−/− retinas in 450-nm light ($p < 9.4 \times 10^{-4}$) and in *Rgr*−/− *Gnat1*−/− in 560-nm light ($p < 4.4 \times 10^{-4}$) compared to *Rgr*+/+ *Gnat1*−/− in 450-nm light. The sensitivities were also significantly lower in *Rgr*−/− *Gnat1*−/− retinas in 560-nm light compared to *Rgr*−/− *Gnat1*−/− retinas in 450-nm light ($p < 0.004$).

by mass action through reduction of 11cRAL to 11cROL by Rdh10. We observed similar redox-photoisomerase activity in microsomes from normal mouse retinas, which was much reduced in microsomes from *Rgr*−/− retinas (Figure 2A). Cultured Müller cells were previously shown to take up atROL and release 11cROL into the medium through an unknown mechanism (Betts-Obregon et al., 2014; Das et al., 1992). Also, bleached cones, but not rods, have been shown to recover light sensitivity upon addition of 11cROL (Goldstein, 1970; Hood and Hock, 1973; Jones et al., 1989). The results presented here suggest that RGR opsin and Rdh10 are the proteins responsible for 11cROL production during light exposure by Müller cells, as depicted in Figure 8.

Since RGR opsin and Rdh10 are also both expressed in RPE cells, we analyzed microsomes from *Rgr*+/+ and *Rgr*−/− RPE for redox-photoisomerase activity. Similar to WT retina microsomes, RPE microsomes also showed light-dependent conversion of atROL to 11cROL (Figures 2A and 2B). These results suggest that RPE cells, in addition to Müller cells, provide 11cROL for light-dependent regeneration of cone pigments.

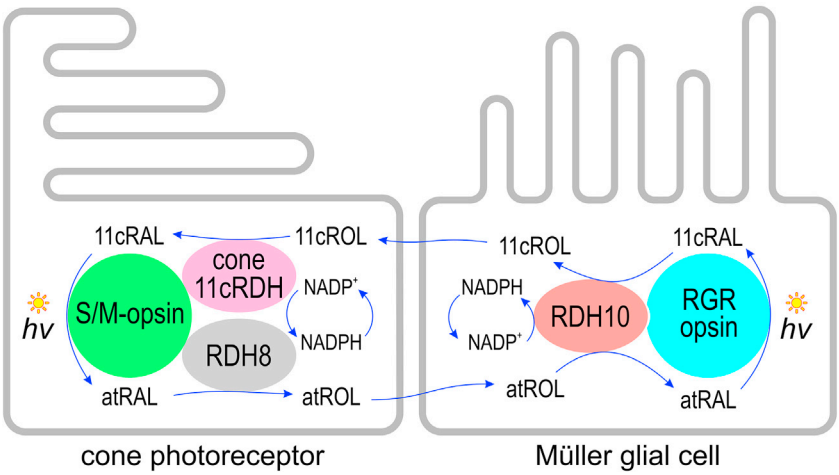

Figure 8. Hypothesized Müller-Cell Visual Cycle

During light exposure, Müller cells take up atROL released by cones and rods (not shown). Rdh10 oxidizes atROL to atRAL, which forms a visual pigment with RGR opsin and is isomerized to 11cRAL upon absorption of a photon (*hv*). The 11cRAL is reduced to 11cROL by Rdh10, balancing the redox reaction in the Müller cell with no net consumption of NADPH or $NADP^+$. The 11cROL is taken up by a cone cell, which contains an as-yet unidentified 11cRDH that oxidizes 11cROL to 11cRAL. The 11cRAL combines with apo-opsin to regenerate the M-opsin pigment. Absorption of a photon (*hv*) by M-opsin activates the visual transduction cascade as the first step in visual perception (not shown). The bleached M-opsin releases atRAL, which is reduced by Rdh8 to atROL, completing the visual cycle.

Thus, RPE cells may contain two visual cycles: the LRAT-Rpe65 pathway (Saari, 2016), and the new pathway defined here by RGR-Rdh10. While RGR opsin is abundant in Müller cells of human (Trifunovic et al., 2008), bovine (Jiang et al., 1993; Pandey et al., 1994), and chicken retinas (Díaz et al., 2017), it is much less abundant in mouse retinas (Tao et al., 1998; Trifunovic et al., 2008) (Figure 3A). Mice are nocturnal animals and, thereby, have less need for a photoisomerase to maintain cone sensitivity under daylight conditions. Despite its low abundance in mouse retinas, we observed robust biochemical (Figure 2) and physiological (Figures 4, 5, and 6) phenotypes in isolated retinas from *Rgr*+/+ versus *Rgr*−/− mice. These results suggest that RGR opsin may however contribute even more to cone pigment regeneration in diurnal animals, such as humans, cows, and chickens, where RGR opsin is more abundant in Müller cells (Díaz et al., 2017; Pandey et al., 1994; Trifunovic et al., 2008).

If the retinoid-isomerase activity of RGR opsin is light dependent, as shown previously for retinaldehyde (Hao and Fong, 1999) and here for retinol (Figures 1A and 1C), why do cones exhibit RGR-dependent recovery in the dark following a photobleach (Figure 6)? The initial phase of post-bleach recovery observed in both *Rgr*+/+ and *Rgr*−/− retinas probably reflects dark adaptation of the visual transduction cascade (Figure 6). The slower, RGR-dependent recovery may reflect regeneration of M-opsin from a storage pool of 11cROL or 11cRAL previously produced by RGR during light exposure. This storage pool may correspond to CRALBP in Müller cells (Bunt-Milam and Saari, 1983), which binds 11cRAL and 11cROL with high affinity but has low affinity for other retinoid isomers (Saari and Bredberg, 1987). In agreement with this notion, cone recovery after light exposure was shown to depend critically on CRALBP in isolated mouse retinas (Xue et al., 2015).

We are used to thinking that visual pigments in vertebrate rods and cones regenerate pigment through a biochemical mechanism involving the enzymatic visual cycle in RPE cells, whereas rhabdomeric photoreceptors of invertebrates use light to regenerate opsin (Fain et al., 2010). This strict dichotomy is no longer valid. Here, we show that cones in mice recover light sensitivity through a photic mechanism involving RGR opsin in Müller cells, in addition to the LRAT-Rpe65 visual cycle in RPE cells. Although this RGR-dependent photic mechanism is different from photoregeneration of bistable opsins in rhabdomeric photoreceptors, it offers the same advantages. With photic regeneration, the rate of chromophore synthesis scales with light intensity, while metabolic regeneration of chromophore is limited by enzyme turnover. Also, conversion of atROL to 11cROL is endergonic (ΔG = +4.1 kcal/mol) (Rando and Chang, 1983). For the LRAT-Rpe65 visual cycle, retinol isomerization comes at the metabolic cost of an activated fatty acid for each absorbed photon (Rando, 1991). Similar to insects and other invertebrates, vertebrates can now claim use of solar energy to power regeneration of cone visual pigment.

STAR★METHODS

Detailed methods are provided in the online version of this paper and include the following:

SUPPLEMENTAL INFORMATION

Supplemental Information can be found online at https://doi.org/10.1016/j.neuron.2019.04.004.

ACKNOWLEDGMENTS

We gratefully acknowledge Henry Fong for providing *Rgr*−/− mice, Janis Lem for the *Gnat1*−/− mice, Andreas Wenzel for the Pin2 and Pin3 anti-RGR Abs, Rosalie Crouch for providing 11cRAL, and Frans Vinberg for help with retinal recording. This work was supported by NEI, National Institutes of Health grants R01-EY024379 (to G.H.T.), R01-EY025002 (to R.A.R.), R01-EY029817 (to A.P.S.), and R01-EY001844 (to G.L.F.); NEI, National Institutes of Health core grant P30-EY000331; and a Research to Prevent Blindness unrestricted grant (to the Jules Stein Eye Institute). G.H.T. is the Charles Kenneth Feldman Professor of Ophthalmology at UCLA.

AUTHOR CONTRIBUTIONS

Conceptualization, G.H.T. and G.L.F.; Methodology, J.J.K., R.F., S.Y.N., A.P.S., R.A.R., G.L.F., and G.H.T.; Formal Analysis, A.M.; Investigation, A.M., J.J.K., A.T., J.J.C., S.Y.N., R.F., T.X., and L.Y.; Resources, A.P.S. and G.H.T.; Writing original draft, G.H.T.; Review and Editing, R.F., A.P.S., R.A.R., and G.L.F.; Supervision, A.P.S., R.A.R, G.L.F., and G.H.T.; Funding acquisition, A.P.S., G.L.F., and G.H.T.

DECLARATION OF INTERESTS

The authors declare no competing interests.

Received: February 7, 2019
Revised: March 20, 2019
Accepted: March 29, 2019
Published: May 2, 2019

REFERENCES

Betts-Obregon, B.S., Gonzalez-Fernandez, F., and Tsin, A.T. (2014). Interphotoreceptor retinoid-binding protein (IRBP) promotes retinol uptake and release by rat Müller cells (rMC-1) in vitro: implications for the cone visual cycle. Invest. Ophthalmol. Vis. Sci. *55*, 6265–6271.

Boettner, E.A., and Wolter, J.R. (1962). Transmission of the ocular media. Invest. Ophthalmol. Vis. Sci. *1*, 776–783.

Bunt-Milam, A.H., and Saari, J.C. (1983). Immunocytochemical localization of two retinoid-binding proteins in vertebrate retina. J. Cell Biol. *97*, 703–712.

Burkhardt, D.A. (1994). Light adaptation and photopigment bleaching in cone photoreceptors in situ in the retina of the turtle. J. Neurosci. *14*, 1091–1105.

Calvert, P.D., Krasnoperova, N.V., Lyubarsky, A.L., Isayama, T., Nicoló, M., Kosaras, B., Wong, G., Gannon, K.S., Margolskee, R.F., Sidman, R.L., et al. (2000). Phototransduction in transgenic mice after targeted deletion of the rod transducin alpha -subunit. Proc. Natl. Acad. Sci. USA *97*, 13913–13918.

Chen, P., Hao, W., Rife, L., Wang, X.P., Shen, D., Chen, J., Ogden, T., Van Boemel, G.B., Wu, L., Yang, M., and Fong, H.K.W. (2001a). A photic visual cycle of rhodopsin regeneration is dependent on Rgr. Nat. Genet. *28*, 256–260.

Chen, P., Lee, T.D., and Fong, H.K.W. (2001b). Interaction of 11-cis-retinol dehydrogenase with the chromophore of retinal g protein-coupled receptor opsin. J. Biol. Chem. *276*, 21098–21104.

Das, S.R., Bhardwaj, N., Kjeldbye, H., and Gouras, P. (1992). Muller cells of chicken retina synthesize 11-cis-retinol. Biochem. J. *285*, 907–913.

Díaz, N.M., Morera, L.P., Tempesti, T., and Guido, M.E. (2017). The visual cycle in the inner retina of chicken and the involvement of retinal G-protein-coupled receptor (RGR). Mol. Neurobiol. *54*, 2507–2517.

Fain, G.L., Hardie, R., and Laughlin, S.B. (2010). Phototransduction and the evolution of photoreceptors. Curr. Biol. *20*, R114–R124.

Farjo, K.M., Moiseyev, G., Takahashi, Y., Crouch, R.K., and Ma, J.X. (2009). The 11-cis-retinol dehydrogenase activity of RDH10 and its interaction with visual cycle proteins. Invest. Ophthalmol. Vis. Sci. *50*, 5089–5097.

Franke, R.R., Sakmar, T.P., Graham, R.M., and Khorana, H.G. (1992). Structure and function in rhodopsin. Studies of the interaction between the rhodopsin cytoplasmic domain and transducin. J. Biol. Chem. *267*, 14767–14774.

Fritze, O., Filipek, S., Kuksa, V., Palczewski, K., Hofmann, K.P., and Ernst, O.P. (2003). Role of the conserved NPxxY(x)5,6F motif in the rhodopsin ground state and during activation. Proc. Natl. Acad. Sci. USA *100*, 2290–2295.

Goldstein, E.B. (1970). Cone pigment regeneration in the isolated frog retina. Vision Res. *10*, 1065–1068.

Govardovskii, V.I., Fyhrquist, N., Reuter, T., Kuzmin, D.G., and Donner, K. (2000). In search of the visual pigment template. Vis. Neurosci. *17*, 509–528.

Haeseleer, F., Jang, G.F., Imanishi, Y., Driessen, C.A.G.G., Matsumura, M., Nelson, P.S., and Palczewski, K. (2002). Dual-substrate specificity short chain retinol dehydrogenases from the vertebrate retina. J. Biol. Chem. *277*, 45537–45546.

Hao, W., and Fong, H.K. (1996). Blue and ultraviolet light-absorbing opsin from the retinal pigment epithelium. Biochemistry *35*, 6251–6256.

Hao, W., and Fong, H.K.W. (1999). The endogenous chromophore of retinal G protein-coupled receptor opsin from the pigment epithelium. J. Biol. Chem. *274*, 6085–6090.

Hood, D.C., and Hock, P.A. (1973). Recovery of cone receptor activity in the frog's isolated retina. Vision Res. *13*, 1943–1951.

Huang, J., Possin, D.E., and Saari, J.C. (2009). Localizations of visual cycle components in retinal pigment epithelium. Mol. Vis. *15*, 223–234.

Jablonski, M.M., and Iannaccone, A. (2000). Targeted disruption of Müller cell metabolism induces photoreceptor dysmorphogenesis. Glia *32*, 192–204.

Jiang, M., Pandey, S., and Fong, H.K. (1993). An opsin homologue in the retina and pigment epithelium. Invest. Ophthalmol. Vis. Sci. *34*, 3669–3678.

Jones, G.J., Crouch, R.K., Wiggert, B., Cornwall, M.C., and Chader, G.J. (1989). Retinoid requirements for recovery of sensitivity after visual-pigment bleaching in isolated photoreceptors. Proc. Natl. Acad. Sci. USA *86*, 9606–9610.

Kaylor, J.J., Yuan, Q., Cook, J., Sarfare, S., Makshanoff, J., Miu, A., Kim, A., Kim, P., Habib, S., Roybal, C.N., et al. (2013). Identification of DES1 as a vitamin A isomerase in Müller glial cells of the retina. Nat. Chem. Biol. *9*, 30–36.

Kaylor, J.J., Cook, J.D., Makshanoff, J., Bischoff, N., Yong, J., and Travis, G.H. (2014). Identification of the 11-cis-specific retinyl-ester synthase in retinal Müller cells as multifunctional O-acyltransferase (MFAT). Proc. Natl. Acad. Sci. USA *111*, 7302–7307.

Kaylor, J.J., Xu, T., Ingram, N.T., Tsan, A., Hakobyan, H., Fain, G.L., and Travis, G.H. (2017). Blue light regenerates functional visual pigments in mammals through a retinyl-phospholipid intermediate. Nat. Commun. *8*, 16.

Kiser, P.D., Kolesnikov, A.V., Kiser, J.Z., Dong, Z., Chaurasia, B., Wang, L., Summers, S.A., Hoang, T., Blackshaw, S., Peachey, N.S., et al. (2019). Conditional deletion of Des1 in the mouse retina does not impair the visual cycle in cones. FASEB J. *33*, 5782–5792.

Leenheer, A.P.d., Lambert, W.E., and Van Bocxlaer, J.F. (2000). Modern Chromatographic Analysis of Vitamins, Third Edition (Marcel Dekker).

Lenis, T.L., Sarfare, S., Jiang, Z., Lloyd, M.B., Bok, D., and Radu, R.A. (2017). Complement modulation in the retinal pigment epithelium rescues photoreceptor degeneration in a mouse model of Stargardt disease. Proc. Natl. Acad. Sci. USA *114*, 3987–3992.

Maeda, T., Van Hooser, J.P., Driessen, C.A., Filipek, S., Janssen, J.J., and Palczewski, K. (2003). Evaluation of the role of the retinal G protein-coupled receptor (RGR) in the vertebrate retina in vivo. J. Neurochem. *85*, 944–956.

Mata, N.L., Radu, R.A., Clemmons, R.C., and Travis, G.H. (2002). Isomerization and oxidation of vitamin a in cone-dominant retinas: a novel pathway for visual-pigment regeneration in daylight. Neuron *36*, 69–80.

Mata, N.L., Ruiz, A., Radu, R.A., Bui, T.V., and Travis, G.H. (2005). Chicken retinas contain a retinoid isomerase activity that catalyzes the direct conversion of all-trans-retinol to 11-cis-retinol. Biochemistry *44*, 11715–11721.

McBean, G.J. (1994). Inhibition of the glutamate transporter and glial enzymes in rat striatum by the gliotoxin, alpha aminoadipate. Br. J. Pharmacol. *113*, 536–540.

Morimura, H., Saindelle-Ribeaudeau, F., Berson, E.L., and Dryja, T.P. (1999). Mutations in RGR, encoding a light-sensitive opsin homologue, in patients with retinitis pigmentosa. Nat. Genet. *23*, 393–394.

Nymark, S., Frederiksen, R., Woodruff, M.L., Cornwall, M.C., and Fain, G.L. (2012). Bleaching of mouse rods: microspectrophotometry and suction-electrode recording. J. Physiol. *590*, 2353–2364.

Pandey, S., Blanks, J.C., Spee, C., Jiang, M., and Fong, H.K. (1994). Cytoplasmic retinal localization of an evolutionary homolog of the visual pigments. Exp. Eye Res. *58*, 605–613.

Radu, R.A., Hu, J., Peng, J., Bok, D., Mata, N.L., and Travis, G.H. (2008). Retinal pigment epithelium-retinal G protein receptor-opsin mediates light-dependent translocation of all-trans-retinyl esters for synthesis of visual chromophore in retinal pigment epithelial cells. J. Biol. Chem. *283*, 19730–19738.

Rando, R.R. (1991). Membrane phospholipids as an energy source in the operation of the visual cycle. Biochemistry *30*, 595–602.

Rando, R.R., and Chang, A. (1983). Studies on the catalyzed interconversion of vitamin A derivatives. J. Am. Chem. Soc. *105*, 2879–2882.

Saari, J.C. (2016). Vitamin A and vision. Subcell. Biochem. *81*, 231–259.

Saari, J.C., and Bredberg, D.L. (1987). Photochemistry and stereoselectivity of cellular retinaldehyde-binding protein from bovine retina. J. Biol. Chem. *262*, 7618–7622.

Sato, S., and Kefalov, V.J. (2016). cis Retinol oxidation regulates photoreceptor access to the retina visual cycle and cone pigment regeneration. J. Physiol. *594*, 6753–6765.

Simon, A., Hellman, U., Wernstedt, C., and Eriksson, U. (1995). The retinal pigment epithelial-specific 11-cis retinol dehydrogenase belongs to the family of short chain alcohol dehydrogenases. J. Biol. Chem. *270*, 1107–1112.

Tao, L., Shen, D., Pandey, S., Hao, W., Rich, K.A., and Fong, H.K. (1998). Structure and developmental expression of the mouse RGR opsin gene. Mol. Vis. *4*, 25.

Trifunovic, D., Karali, M., Camposampiero, D., Ponzin, D., Banfi, S., and Marigo, V. (2008). A high-resolution RNA expression atlas of retinitis

pigmentosa genes in human and mouse retinas. Invest. Ophthalmol. Vis. Sci. *49*, 2330–2336.

Vinberg, F., Kolesnikov, A.V., and Kefalov, V.J. (2014). Ex vivo ERG analysis of photoreceptors using an in vivo ERG system. Vision Res. *101*, 108–117.

Wang, J.S., and Kefalov, V.J. (2009). An alternative pathway mediates the mouse and human cone visual cycle. Curr. Biol. *19*, 1665–1669.

Wang, J.S., Nymark, S., Frederiksen, R., Estevez, M.E., Shen, S.Q., Corbo, J.C., Cornwall, M.C., and Kefalov, V.J. (2014). Chromophore supply rate-limits mammalian photoreceptor dark adaptation. J. Neurosci. *34*, 11212–11221.

Wenzel, A., Oberhauser, V., Pugh, E.N., Jr., Lamb, T.D., Grimm, C., Samardzija, M., Fahl, E., Seeliger, M.W., Remé, C.E., and von Lintig, J. (2005). The retinal G protein-coupled receptor (RGR) enhances isomerohydrolase activity independent of light. J. Biol. Chem. *280*, 29874–29884.

Woodruff, M.L., Lem, J., and Fain, G.L. (2004). Early receptor current of wild-type and transducin knockout mice: photosensitivity and light-induced Ca2+ release. J. Physiol. *557*, 821–828.

Wu, B.X., Chen, Y., Chen, Y., Fan, J., Rohrer, B., Crouch, R.K., and Ma, J.X. (2002). Cloning and characterization of a novel all-trans retinol short-chain dehydrogenase/reductase from the RPE. Invest. Ophthalmol. Vis. Sci. *43*, 3365–3372.

Wu, B.X., Moiseyev, G., Chen, Y., Rohrer, B., Crouch, R.K., and Ma, J.X. (2004). Identification of RDH10, an all-trans retinol dehydrogenase, in retinal Muller cells. Invest. Ophthalmol. Vis. Sci. *45*, 3857–3862.

Xue, Y., Shen, S.Q., Jui, J., Rupp, A.C., Byrne, L.C., Hattar, S., Flannery, J.G., Corbo, J.C., and Kefalov, V.J. (2015). CRALBP supports the mammalian retinal visual cycle and cone vision. J. Clin. Invest. *125*, 727–738.

STAR★METHODS

KEY RESOURCES TABLE

REAGENT or RESOURCE	SOURCE	IDENTIFIER
Antibodies		
Rabbit polyclonal anti-RGR	Andreas Wenzel	Pin 3
Guinea pig polyclonal anti-RGR	Andreas Wenzel	Pin 2
IRDye 800CW donkey anti-guinea pig antibody	LI-COR	926-32411
Mouse Monoclonal ANTI-FLAG® M2 antibody	Sigma-Aldrich	F3165
Mouse anti-Myc Tag Antibody, clone 4A6	Millipore Sigma	05-724
Donkey anti-Mouse 800 secondary antibody IgG (H+L)	Li-COR	926-32212
Mouse monoclonal RLBP-1 (clone 1H7) antibody	Sigma-Aldrich	WH0006017M1
Goat anti-Rabbit IgG (H+L) secondary antibody, Alexa Fluor 488	Thermo Fisher	A-11008
Goat anti-mouse IgG (H+L) secondary antibody, Alexa Fluor 568	Thermo Fisher	A-11004
Chemicals, Peptides, and Recombinant Proteins		
All-*trans*-retinol	Sigma-Aldrich	95144; CAS# 68-26-8
Bovine serum albumin	Sigma-Aldrich	A6003; CAS# 9048-46-8
Polyfect™ Transfection Reagent	QIAGEN	301107
Hydroxylamine hydrochloride	Sigma-Aldrich	255580; CAS# 5470-11-1
Hexanes	Thermo Fisher	H303-4; CAS# 110-54-3
1,4-dioxane	Sigma-Aldrich	34857; CAS# 123-91-1
Ames' medium	Sigma-Aldrich	A1420
Sodium bicarbonate	Sigma-Aldrich	S6014; CAS# 144-55-8
L-aspartic acid	Sigma-Aldrich	A9256; CAS# 56-84-8
DL-2-amino-4-phosphonobutyric acid	Tocris Bioscience	0101; CAS# 20263-07-4
Sodium L-lactate	Sigma-Aldrich	71718; CAS# 867-56-1
Benzonase nuclease	Sigma-Aldrich	E1014-25KU; CAS# 9025-65-4
Halt protease inhibitor cocktail (100X)	Thermo Scientific	78429
Micro BCA protein assay kit	Thermo Scientific	23235
NuPAGE LDS sample buffer (4X)	Novex (Life Technologies)	NP0007
NuPAGE sample reducing agent (10X)	Novex (Life Technologies)	NP0009
NuPAGE 12% Bis-Tris gel	Novex (Life Technologies)	NP0342BOX
Immobilon-FL transfer membrane	Merck Millipore	IPFL00010
Odyssey blocking buffer™ (PBS)	LI-COR	927-40000
Donkey serum	Sigma-Aldrich	D9663-10ML
Anased xylazine injection solution	Akorn	NADA# 139-236
Ketamine hydrochloride	Putney	NADA# 26637-731-51
DMEM (phenol free)	Thermo Fisher	21063-029
Penicillin-streptomycin	Thermo Fisher	15070-063
BCA Protein Assay Kit	Thermo Fisher	23225
Sodium dodecyl sulfate (SDS)	Sigma-Aldrich	L3771; CAS# 151-21-3
Fetal bovine serum	Thermo Fisher	16140-071
Nicotinamide adenine dinucleotide phosphate (reduced)	Sigma-Aldrich	N7505; CAS# 2646-71-1
Protein G Dynabeads™ immunoprecipitation kit	Thermo Fisher	10007D
TRIS base	Thermo Fisher	BP152; CAS# 77-86-1
Sodium chloride	Thermo Fisher	S271-500; CAS# 7647-14-5
Glycerol	Thermo Fisher	G33-500; CAS# 56-81-5

(*Continued on next page*)

Continued		
REAGENT or RESOURCE	SOURCE	IDENTIFIER
NP-40 detergent Surfact-Amps™ solution	Thermo Fisher	28324: CAS# 9016-45-9
Phosphate buffered saline (PBS)	Thermo Fisher	20012-050
Tween 20	Thermo Fisher	BP337-500; CAS# 9005-64-5
Sodium borohydride	Sigma-Aldrich	213462; CAS# 16940-66-2
Triton X-100	Sigma-Aldrich	T-9284; CAS# 9002-93-1
normal goat serum	Sigma-Aldrich	G9023
Prolong Gold antifade reagent with DAPI mounting solution	Thermo Fisher	P36935
Experimental Models: Cell Lines		
HEK293T Cell Line	ATCC	CRL-11268
Experimental Models: Organisms/Strains		
Mouse: *Rgr* −/−	Henry Fong Lab	University of Southern California
Mouse: *Gnat1* −/−	Janis Lem	Tufts University, Boston
Mouse: *Rgr* −/− / *Gnat1* −/− double knock-out	This paper	N/A
Mouse: wild-type 129S6/SvEv Tac	Taconic Biosciences	TAC 129SVE
Oligonucleotides		
(*Rd8*): forward-5′GGTGACCAATCTGTTGACAATCC	PMID: 22447858	N/A
(*Rd8*): reverse-5′GCCCCATTTGCACACTGATGAC	PMID: 22447858	N/A
(*Rpe65 codon 450*): forward- 5′CCTTTGAATTTCCTCAAATCAATTA	PMID: 18474598	N/A
(*Rpe65 codon 450*): reverse- 5′TTCCAGAGCATCTGGTTGAG	PMID: 18474598	N/A
(*Gnat1*−/−): WT forward- 5′GTTCATTGCCATCATCTACGG	PMID: 11095744	N/A
(*Gnat1*−/−): WT reverse- 5′GCATTGTGCCTTCCTCAATAG	PMID: 11095744	N/A
(*Gnat1*−/−): KO forward- 5′AGCACAGCTTTCCTTTCAGG	PMID: 11095744	N/A
(*Gnat1*−/−): KO reverse- 5′CAGAAAGCGAAGGAGCAAAG	PMID: 11095744	N/A
(*RGR*−/−): forward ('RGR-Oligo1')- 5′TGCATTTTCCTGTGAGATGG	PMID: 18474598	N/A
(*RGR*−/−): reverse ('RGR-Oligo2′)- 5′GCTCAGTACCAGCAGGTTGC	PMID: 18474598	N/A
(*RGR*−/−): reverse ('RGR-Oligo3′)- 5′GGGGAACTTCCTGACTAGGG	PMID: 18474598	N/A
Recombinant DNA		
Plasmid: pcDNA 3.1+	Thermo Fisher	V79020 (vector for all constructs)
Human RDH5	Genscript	NM_001199771.1
Human RDH8	Genscript	NM_015725.2
Human RDH10	Genscript	NM_172037.5
Human RDH14	Genscript	NM_020905.4
Chicken RDH10	Genscript	NM_001199459.1
Human RDH11	Krzysztof Palczewski	NM_016026.4
Mouse RDH10	Origene	NM_133832.3
Bovine RDH10	Genscript	NM_174734.2
Bovine RGR	Genscript	NM_175775.2
Chicken RGR	Genscript	NM_001031216.1
Software and Algorithms		
SigmaPlot (biochemistry data)	Systat Software Inc.	http://www.sigmaplot.co.uk/products/sigmaplot/sigmaplot-details.php
OriginPro (physiology data)	OriginLab	http://www.originlab.com/origin

CONTACT FOR REAGENT AND RESOURCE SHARING

Further information and requests for resources and reagents should be directed to and will be fulfilled by the lead contact, Gabriel H. Travis (travis@jsei.ucla.edu).

EXPERIMENTAL MODEL AND SUBJECT DETAILS

Animal use and care statement

This study was carried out in accordance with the recommendations in the Guide for the Care and Use of Laboratory Animals of the National Institutes of Health, and the Association for Research in Vision and Ophthalmology Statement for the Use of Animals in Ophthalmic and Vision Research. The animal use protocol was approved by the University of California, Los Angeles Animal Research Committee (Permit Number: A3196-01). Euthanasia was performed by cervical dislocation in deeply anesthetized mice by intraperitoneal injections (xylazine 10 mg/kg and ketamine 100 mg/kg). All efforts were made to minimize pain and discomfort in mice used in this study.

Mice and Genotyping

All mice were reared under 12-hour cyclic light. *Rgr*−/− mice were generously provided by Henry Fong. The genotyping protocol was as previously reported (Radu et al., 2008). Wild-type (129/Sv) mice were purchased from Taconic Biosciences, Inc. All mice used were tested to exclude the spontaneous *Rd8* and *Rpe65*-M450 mutations using the primers (*Rd8*): forward-5′GGTGACCAAT CTGTTGACAATCC and reverse-5′GCCCCATTTGCACACTGATGAC; and (*Rpe65*): forward-5′CCTTTGAATTTCCTCAAATCAATTA and reverse-5′TTCCAGAGCATCTGGTTGAG. To determine the genotype at *Gnat1*, we used the wild-type primer set: forward-5′GTTCATTGCCATCATCTACGG and reverse-5′GCATTGTGCCTTCCTCAATAG; and the knockout

primer set: forward-5′AGCACAGCTTTCCTTTCAGG and reverse-5′CAGAAAGCGAAGGAGCAAAG. To determine the genotype at *Rgr*, we used the multiplexed wild-type and knockout primer set forward-5′TGCATTTTCCTGTGAGATGG ('RGR-oligo1'), reverse-5′GCTCAGTACCAGCAGGTTGC ('RGR-oligo2′), and reverse-5′GGGGAACTTCCTGACTAGGG ('RGR-oligo3′). For enzymatic assays, retina and RPE-containing eyecups were isolated from the eyes of two-month-old wild-type (129/Sv) and *Rgr*−/− mice of both sexes.

HEK293T Cells

Authenticated human female embryonic kidney epithelial cells were purchased from ATCC (HEK293T/17; CRL-11268). Cells were grown and maintained in DMEM (GIBCO/Thermofisher) supplemented with 10% heat-inactivated fetal bovine serum and antibiotics (100 U/mL of penicillin G and 100 μg/mL of streptomycin) at 37°C in 5% CO_2. These cells constitutively express the simian virus 40 (SV40) large T antigen and clone 17 was selected specifically for its high transfectability.

METHOD DETAILS

General enzyme assay conditions

All experimental manipulations involving retinoids were performed in a darkroom under dim red light. Protein samples and solutions were kept on ice until use. Stocks of atROL were freshly dissolved in ethanol and stored on ice. Stock concentration was determined by UV-VIS spectroscopy using the reported extinction coefficient (ε) for all-*trans*-ROL (λ_{max} = 325 nm, ϵ = 52,770 $M^{-1}cm^{-1}$) (Leenheer et al., 2000). Unless otherwise stated, all chemicals and solvents were purchased from Sigma-Aldrich. Protein concentrations were measured using the Micro BCA Protein Assay Kit (Pierce).

Normal-phase HPLC analysis of retinoids

Retinoids were extracted from assay mixtures after quenching the reactions with methanol (2 mL) followed by addition of 25 μL 5% SDS (0.2% SDS final concentration) and brine (50 μL). To protect retinaldehydes, retinal oximes were generated by addition of hydroxylamine hydrochloride (500 μL of 1.0 M solution) (Sigma), vortexing, and incubation at room temperature for 15 min. The samples were then twice extracted by addition of two mL aliquots of hexane followed by brief vortexing and centrifugation at 3000 x g for five minutes to separate phases. Pooled hexane extracts were added to 13 × 100 mm borosilicate test tubes and evaporated to dryness under a stream of nitrogen. Dried samples were then dissolved in 115 μL hexane and analyzed by normal-phase liquid chromatography in an Agilent 1100 series chromatograph equipped with a photodiode-array detector using an Agilent Zorbax RX-SIL column (4.6 × 100 mm, 1.8 μM) using a 0.24%–10% dioxane gradient in hexane, at a flow rate of 0.9 mL per minute. Spectra (190-550 nm) were acquired for all eluted peaks. The identity of each eluted peak was established by comparing its spectrum and elution time with those of authentic retinoid standards. Sample peaks were quantitated by comparing peak areas to calibration curves established with retinoid standards.

Activity of RGR and RDH10 in dark versus light

Bovine RDH10 (NM_174734.2) and bovine RGR (NM_175775.2) cDNA's were synthesized by GenScript and subcloned into the mammalian expression vector, pcDNA 3.1 (ThermoFisher). HEK293T cells were grown in DMEM (GIBCO/Thermofisher) supplemented with 10% heat-inactivated fetal bovine serum and antibiotics (100 U/mL of penicillin G and 100 μg/mL of streptomycin) at 37°C in 5% CO_2. HEK293T cells were transfected (PolyFect, QIAGEN) with non-recombinant pcDNA3.1, pcDNA3.1-RDH10, and/or pcDNA3.1-RGR. When more than one type of clone were used, the transfection were done with equal amounts (50/50) of plasmid. After approximately 40 hours in culture, the medium above the cells was removed and replaced with phenol red-free

DMEM (GIBCO/ThermoFisher: 21063-029) supplemented with 5 μM atROL, 2% bovine serum albumin (BSA), and 250 μM NADPH. Plates were placed in a 37°C incubator and exposed for 30 min to monochromatic light (470nm ± 10nm at 0.4 W/m^2) or kept in the dark. The light wavelength and intensity was measured with a spectroradiometer (Black-comet CXR-SR-50, StellarNet Inc.) The monochromatic light was generated by a custom monochromator (Newport Instruments) with a xenon arc lamp. After each assay, the media was separated from the cells by centrifugation (five minutes at 1,000 rpm in a Sorvall Legend RT). The media were extracted as described above for retinoid analysis.

Immunoblot analysis

The immunoblot analysis was performed following similar methods previously published (Kaylor et al., 2013; Lenis et al., 2017). Retinas and RPE-containing eyecups were dissected from euthanized 129/Sv (*Rgr*+/+) and *Rgr*−/− mice (about 12-14 weeks old), and homogenized in 1X PBS (pH 7.2) with Halt protease inhibitor cocktail on ice. The homogenates were treated with benzonase nuclease for one hour at room temperature followed by 1% (final concentration) SDS at 4°C for 20 min. The treated homogenates were centrifuged at 3,000 x g for 5 min and the supernatants were collected and stored at −80°C for further analysis. The total protein concentration of each sample was determined by a micro BCA protein assay (Thermo Scientific) according to the protocol suggested by the manufacturer. Protein samples were heat-denatured in NuPAGE LDS sample buffer and NuPAGE sample reducing agent, and then separated by a NuPAGE 12% Bis-Tris gel (Novex by Life Technologies). Proteins were transferred to an Immobilon-FL PVDF transfer membrane (Merck Millipore) using a Trans-Blot SD semi-dry transfer cell (BIO-RAD). The blot/membrane was blocked in Odyssey blocking buffer and probed with a guinea pig anti-RGR ('Pin2′) primary antibody (courtesy of Andreas Wenzel) at 1:1000 dilution followed by an IRDye 800CW donkey anti-guinea pig (LI-COR) secondary antibody at 1:15000 dilution in Odyssey blocking buffer with 0.1% Tween 20 and 0.5% donkey serum. The blot/membrane was imaged by an Odyssey CLx Infrared Imaging System (LI-COR).

Immunocytochemistry of mouse retina sections

Eyes were enucleated and fixed in 2% PFA in 0.1M sodium phosphate buffer for one hour. Eyecups were prepared by removal of anterior segments then infiltrated with 10%–30% sucrose, embedded in OCT, and cut into 18-μm sections. Sections were reduced in 0.1 M $NaBH_4$, washed in PBS, permeabilized with 0.1% Triton x-100, and blocked with 1% BSA and 5% normal goat serum. Slides were probed overnight at 4°C with rabbit polyclonal anti-RGR 'Pin3′ (red) and mouse monoclonal anti-RLBP-1 clone 1H7 (green). All sections were washed and incubated with Alexa Fluor secondary antibodies for two hours at room temperature. Slides were mounted with ProLong Gold antifade reagent containing DAPI. Images were obtained using Olympus FluoView FV1000 confocal microscope under a 40x oil objective.

Activity of RGR with different RDH's in the retina

Human RDH5 (NM_001199771.1), RDH8 (NM_015725.2), RDH10 (NM_172037.4), and RDH14 (NM_020905.3), as well as chicken RDH10 (NM_001199459.1), were synthesized by GenScript and placed in mammalian expression vector pcDNA 3.1 (ThermoFisher). Mouse RDH10 (NM_133832.3; Origene) and human RDH11 (NM_016026.3; generously provided by Krzysztof Palczewski) were also placed in the mammalian expression vector pcDNA 3.1. Retinol dehydrogenase clones were transfected as described above into HEK293T cells with bovine RGR (50/50 plasmid mix). Background controls were transfected by replacing the RDH clone with non-recombinant pcDNA3.1 (RGR only control) or by transfecting the cells only with pcDNA 3.1 (cell background control). After culturing for approximately 40 hours to express proteins, the media were changed as described above. All plates were exposed to 30 min of monochromatic light (470nm ± 10nm at 0.4 W/m^2) and treated as described above for retinoid analysis.

Action Spectrum of Bovine RGR/RDH10 Activity

HEK293T cells were transfected (PolyFect, QIAGEN) with five μg each of pcDNA3.1-bRDH10 and pcDNA3.1-bRGR plasmid. After ~40 hours the media were replaced with phenol red-free DMEM supplemented with five μM atROL and 2% bovine serum albumin (BSA) (Sigma). The plates were either kept in the dark or illuminated with monochromatic light at wavelengths of 425 to 575 nm with 20-30 nm increments at 37°C for 30 min. The monochromatic light was generated by monochromator and measured by spectroradiometer as described above. The light intensities were adjusted (from 0.35 W/m^2 at 425 nm to 0.26 W/m^2 at 575 nm) such that each wavelength delivered the same photon flux. The media were extracted as described above and analyzed for retinoid content.

Retinoid Photoisomerization in Mouse Retina and RPE Microsomes

Retina and RPE-containing eyecups were isolated from the eyes of two-month-old wild-type (129/Sv) and *Rgr*−/− mice. Identical tissues were combined and homogenized in 500 μl mL of pH 7.0 phosphate citrate (PC) buffer (Sigma) for each mouse strain using glass-glass homogenizers (Kontes). The bulk homogenates were pelleted at 15,000 x g (Eppendorf 5424 centrifuge) for five minutes at 4°C. The S1-supernatants were collected and re-spun at 100,000 g (Sorvall M-150 ultra-centrifuge) for 60 min at 4°C. The S2-supernatants were discarded and the P2-pellets were resuspended in 3.5 mL of PC buffer. Samples of each microsome preparation were used for protein determinations. Triplicate aliquots containing 500 μL of microsomes plus 2% BSA and 5 μM atROL were used in the assays. One set of samples was immediately extracted to determine the content of retinoids before light exposure in order to ascertain the endogenous retinoid profile. The other samples were placed in cuvettes and agitated, exposed to monochromatic

light (470 nm ± 10nm at 0.4 W/m^2) for 30 min at 37°C. Retinoids were extracted and analyzed by normal-phase HPLC as described above. The remaining 11cROL and 11cRAL levels reflect retinoids synthesized during light exposure in microsomes from wild-type and *Rgr−/−* retinas.

Electrophysiology

We used mice between 3 and 6 months of age indiscriminently from either sex. Eyes were enucleated under dim red light or in darkness by means of infrared goggles (American Technologies Network Corporation, San Francisco, CA, USA). The anterior portion of the eye was cut and the lens and cornea were removed in darkness with a dissection microscope. The retina was isolated from the eyecup, and the retinal pigment epithelium was removed with fine tweezers. The retina was then mounted on filter paper (Millipore, 0.45 μm), on the bottom compartment of a perfusion chamber (Vinberg et al., 2014), with the photoreceptor side up in complete darkness. One Ag/AgCl pellet electrode was placed in contact with electrode solution on ganglion cell side of the retina, and another was placed in the solution bathing the photoreceptors. The electrodes were connected to a differential amplifier (Warner instruments DP-311).

During recording, the photoreceptors were continuously perfused with Ames' medium (Sigma Chemical, St Louis, MO, USA), containing an additional 1.9 g/l $NaHCO_3$ and equilibrated with 95% O_2 / 5% CO_2. This solution was supplemented with 2 mM aspartic acid, 40 μM DL-2-amino-4-phosphonobutyric acid (AP4, Tocris Bioscience, Bristol, UK), 4 mM L-lactate, and 10 μM atROL in 0.05% bovine serum albumin (Sigma). The osmolarity of the medium was adjusted to 284 mOsm with a vapor-pressure osmometer (Wescore, Logan, UT). Temperature was maintained at 36–38°C with an automatic temperature controller (Warner instruments, Hamden, CT).

Illumination was delivered with an OptoLED optical system (Cairn Research, Faversham, UK) coupled to an inverted microscope. The 565-nm test flashes and 505-nm background were produced by monochromatic LEDs at the appropriate wavelengths, but the 450-nm and 560-nm illuminations were provided by a white LED coupled to 10-nm-bandwidth interference filters (Andover Corp, Salem, NH), as in previous experiments (Kaylor et al., 2017). The intensities of the test and bleaching lights were calibrated with a photodiode (OSI Optoelectronics, Hawthorne, CA), and the intensities of the 450-nm and 560-nm background lights were set to the same number of photons by adjusting the current of the white LED. To calculate the number of pigment molecules bleached by this illumination, we compared the number of photons per μm^2 required to produce a half-maximal response ($I_{½}$) of single dark-adapted mouse M cones in retinal slices (Kaylor et al., 2017) with the $I_{½}$ of the dark-adapted M-cone response of whole retina (Figure 2). The ratio was then multiplied by the collecting area of the cones, referenced to the collecting area of rods obtained from single-photon responses in slice recordings. Our value of 0.105 is close to that obtained by Vinberg and coworkers (Vinberg et al., 2014). Recordings were filtered and sampled at 1 kHz. Data were displayed and analyzed with PCLAMP (Molecular Devices, Sunnyvale, CA) and Origin Plotting software (OriginLabs, Cambridge, MA).

Pigment bleaching was achieved by illuminating the isolated retina inside the recording chamber. The fraction of pigment bleached is independent of the photoreceptor collecting area and could be estimated from: $F = 1 - exp(-IPt)$, where F is the fraction bleached, I is the intensity of the bleaching light, t is the time of exposure of the bleaching light, and P is the *in situ* photosensitivity of vertebrate photopigment (5.7×10^{-9} μm^2), (Nymark et al., 2012; Woodruff et al., 2004). It is important to note that the use of this equation assumes that there was no pigment regeneration.

QUANTIFICATION AND STATISTICAL ANALYSIS

Production of 11cROL and 11cRAL from atROL by RGR and RDH10 co-expressing cells in 470 nm light was analyzed by one-way ANOVA with Tukey's post hoc analysis. Each bar represents n = 3 plates of transfected cells. Data represent mean ± SD; n.s., not significant, * $p < 0.05$, ** $p < 0.01$, *** $p < 0.001$.

The action spectrum of bovine RGR with bovine RHD10 was analyzed by one-way ANOVA with Tukey's post hoc analysis. Each bar represents n = 3 plates of transfected cells. Data represent mean ± SD; n.s., not significant, * $p < 0.05$, ** $p < 0.01$, *** $p < 0.001$.

RGR knockout mouse microsome photoisomerase activity was analyzed by one-way ANOVA with Tukey's post hoc analysis. Each bar represents n = 3 samples of microsomes. Data represent mean ± SD; n.s., not significant, * $p < 0.05$, ** $p < 0.01$, *** $p < 0.001$.

Differences in sensitivity and maximum amplitude of physiological recordings were tested with two-factor ANOVA including interactions. For Figures 5 and 7 we compared responses at 15, 30, 45, and 60 minutes; and for Figure 6, at 5, 15, 30 and 60 minutes. The values of the reported probabilities *p* for these comparisons are given in the figure legends. The *p* values for interaction were uniformly greater than 0.1 and not significant.